Civil and Environmental Engineering Faculty Works

Civil and Environmental Engineering

2017

Improving the simulation of large lakes in regional climate modeling: Two-way lake-atmosphere coupling with a 3D hydrodynamic model of the Great Lakes

Pengfei Xue

Jeremy S. Pal
Loyola Marymount University, jpal@lmu.edu

Xinyu Ye

John D. Lenters

Chenfu Huang

See next page for additional authors

Authors

Pengfei Xue, Jeremy S. Pal, Xinyu Ye, John D. Lenters, Chenfu Huang, and Philip Y. Chu

Improving the Simulation of Large Lakes in Regional Climate Modeling: Two-Way Lake–Atmosphere Coupling with a 3D Hydrodynamic Model of the Great Lakes

Pengfei Xue,[a,b] Jeremy S. Pal,[c] Xinyu Ye,[a,b] John D. Lenters,[d,f] Chenfu Huang,[a,b]
and Philip Y. Chu[e]

[a] Great Lakes Research Center, Michigan Technological University, Houghton, Michigan
[b] Department of Civil and Environmental Engineering, Michigan Technological University, Houghton, Michigan
[c] Department of Civil Engineering and Environmental Science, Seaver College of Science and Engineering,
Loyola Marymount University, Los Angeles, California
[d] LimnoTech, Ann Arbor, Michigan
[e] NOAA/Great Lakes Environmental Research Laboratory, Ann Arbor, Michigan

(Manuscript received 17 March 2016, in final form 12 September 2016)

ABSTRACT

Accurate representations of lake–ice–atmosphere interactions in regional climate modeling remain one of the most critical and unresolved issues for understanding large-lake ecosystems and their watersheds. To date, the representation of the Great Lakes two-way interactions in regional climate models is achieved with one-dimensional (1D) lake models applied at the atmospheric model lake grid points distributed spatially across a 2D domain. While some progress has been made in refining 1D lake model processes, such models are fundamentally incapable of realistically resolving a number of physical processes in the Great Lakes. In this study, a two-way coupled 3D lake-ice–climate modeling system [Great Lakes–Atmosphere Regional Model (GLARM)] is developed to improve the simulation of large lakes in regional climate models and accurately resolve the hydroclimatic interactions. Model results are compared to a wide variety of observational data and demonstrate the unique skill of the coupled 3D modeling system in reproducing trends and variability in the Great Lakes regional climate, as well as in capturing the physical characteristics of the Great Lakes by fully resolving the lake hydrodynamics. Simulations of the climatology and spatiotemporal variability of lake thermal structure and ice are significantly improved over previous coupled, 1D simulations. At seasonal and annual time scales, differences in model results are primarily observed for variables that are directly affected by lake surface temperature (e.g., evaporation, precipitation, sensible heat flux) while no significant differences are found in other atmospheric variables (e.g., solar radiation, cloud cover). Underlying physical mechanisms for the simulation improvements using GLARM are also discussed.

Corresponding author e-mail: Pengfei Xue, pexue@mtu.edu

1. Introduction

Consisting of five large lakes, the Great Lakes of North America (also known as the Laurentian Great Lakes) form the largest surficial area of freshwater on Earth. The total surface area of the Great Lakes covers approximately $245\,000\,\text{km}^2$, spanning approximately 16° of longitude and 7.5° of latitude (Fig. 1). The Great Lakes contain $23\,000\,\text{km}^3$ of freshwater, holding one-fifth of the world's surface freshwater by volume. Lake depth varies significantly, from a few meters in the coastal regions to a few hundred meters in the deep basins, with the deepest location being roughly 400 m in southeastern Lake Superior (Table 1). Because of their sealike characteristics
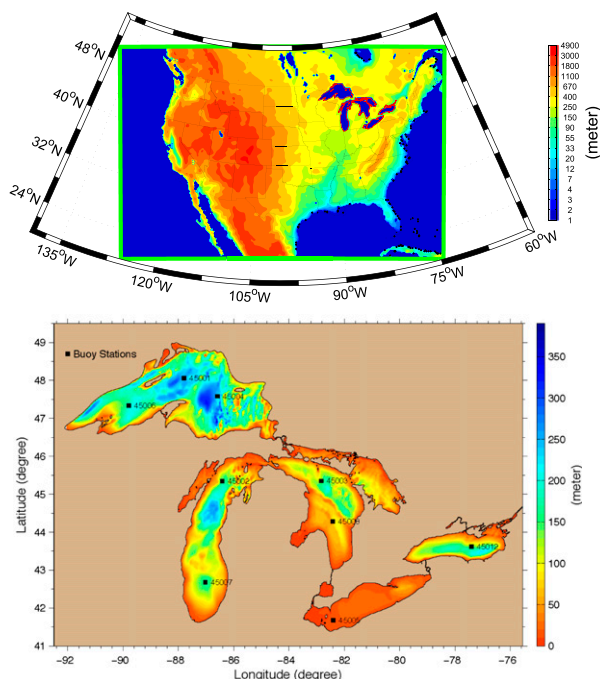
FIG. 1. (top) North American RCM model domain with topography. (bottom) Bathymetry of the North American Great Lakes with NDBC buoy station locations (black squares).

TABLE 1. Morphometric information for the Great Lakes.

	Lake Superior	Lake Michigan	Lake Huron	Lake Ontario	Lake Erie
Average depth (m)	149	85	59	86	19
Maximum depth (m)	406	281	229	244	64
Volume (km³)	12 232	4918	3538	1639	483
Water surface area (km²)	82 097	57 753	59 565	19 009	25 655

(distant horizons, great depths, steep bathymetric gradients, rolling waves, sustained winds, strong Coriolis-influenced currents, and large thermal variability), the Great Lakes have long been referred to as "inland seas," playing a critical role in the variability of the hydroclimatic system throughout the Great Lakes region (Williamson 1854).

The Great Lakes are not only sensitive to climate change, which is likely to have contributed to recent large fluctuations in lake level, thermal structure, and ice coverage, but they are also a significant regional climate driver because of their large volume, thermal inertia, and surface area (Wang et al. 2012; Clites et al. 2014b; Van Cleave et al. 2014; Gronewold et al. 2015). Each of these factors contributes to strong linkages between air and lake temperature, evaporation, precipitation, and ice coverage in the coupled regional lake–atmosphere system (Blanken et al. 2011; Lenters et al. 2013). Lake surface temperature (LST) and ice coverage have a strong impact on regional climate. They also serve as physical indicators of climate change through direct interactions with surface winds and atmospheric heat and moisture fluxes, which in turn modify the lakes' thermal structure, water level, and circulation, making the system particularly sensitive to climate change. For example, warmer winters, loss of ice coverage, and earlier summer stratification of Lake Superior have caused summer LSTs to warm faster

than summer air temperatures in recent decades (Austin and Colman 2007), while the reverse has been observed in winter, with air temperatures warming faster than winter LSTs (Lenters 2004). Rapid summer LST warming has also been seen in other deep lakes around the world (Huang et al. 2012; O'Reilly et al. 2015; Zhong et al. 2016). In addition, large interannual variations in winter air temperatures and ice coverage on the Great Lakes have been observed recently within only a 3-yr time span, often referred to as the "big heat" of 2012 and "big chill" of 2014, leading to significant impacts on water temperature, evaporation, and lake levels in the subsequent ice-free seasons (Wang et al. 2012; Lenters et al. 2013; Clites et al. 2014b; Gronewold et al. 2015). This has brought renewed attention to the future impacts of large trends and strong climatic variability on the Great Lakes. Nevertheless, the complexities of the thermal structure, ice distribution, and circulation patterns in these large "inland seas" make the prediction of such impacts extremely challenging.

Climate models are the primary tool used to assess climate change and associated impacts (IPCC 2013). Despite the significant effects of the Great Lakes on the regional climate, only a few of the atmosphere–ocean general circulation models (AOGCMs) from phase 5 of the Coupled Model Intercomparison Project (CMIP5) used in the latest IPCC report (IPCC 2013) provide even crude representations of the lakes (less than 20 grid points for the Great Lakes); the remaining AOGCMs treat the lakes as land points. Regional climate models (RCMs) aim to enhance regional detail in response to regional-scale forcing through a more realistic representation of physics and dynamics by including finer-scale topography, vegetation, and land/water coverage (Feser et al. 2011; Giorgi 2006). The finer grid resolution (tens of kilometers) generally improves simulations of regional climate and provides more detailed characteristics of temperature, wind, moisture, and precipitation in comparison to global reanalysis datasets and AOGCM simulations. To date, the most common coupled representations of the Great Lakes region are performed using RCMs coupled with

one-dimensional (1D) lake models at RCM lake grids [i.e., 1D lake models are distributed spatially across a two-dimensional (2D) domain to form a three-dimensional (3D) representation of a lake: RCM coupled with 1D lake models] (Hostetler et al. 1993; Lofgren 2004; Subin et al. 2012; Notaro et al. 2013). Although considerable progress has been made in refining the 1D deep-lake model processes, primarily through an improved characterization of vertical mixing and eddy diffusivity (Subin et al. 2012; Bennington et al. 2014; Lofgren 2014), Bennington et al. (2014) point out that "although the Hostetler lake model within RegCM4 is now able to capture a reasonable vertical structure of temperature, circulation and dynamics must be accounted for in large, deep lakes." Other studies applying RCMs with 1D lake models to the Great Lakes region also recognize the need for 3D lake models to accurately represent the physical characteristics of the Great Lakes and properly resolve horizontal and vertical mixing processes to reduce biases in LST, ice coverage, and thermal stratification in regional climate simulations (e.g., Lofgren 2004; Gula and Peltier 2012; Notaro et al. 2013).

Studies in other regions also report that traditional modeling approaches that neglect lake hydrodynamics and consider thermodynamics alone are not satisfactory. For example, Song et al. (2004) found that not including the wind-driven transport of heat from warm regions of Lake Victoria to cooler regions within the lake results in a degraded simulation of the climate downstream, not only over the rest of the lake but also over the surrounding land regions. The resulting asymmetric LST distribution modifies the overlying wind circulation, cloud cover, and rainfall. Only a 3D lake model coupled with an RCM resolves this secondary feature through explicit lake–atmosphere interactions.

All of these research concerns point to the urgency of properly resolving large-lake hydrodynamics and interactions with the overlying atmosphere for improving regional climate modeling of the Great Lakes. The most suitable approach is to represent the system through two-way coupling of a regional climate model with a 3D hydrodynamic model. This is the current direction of next-generation model development and the most likely method for obtaining reliable projections of the future impacts of climatic trends and interannual variability on the Great Lakes system from a regional modeling perspective. Thus, the purpose of this paper is to introduce such a two-way coupled modeling system for the Great Lakes, including demonstration of the reliable skill of the model in simulating large-lake hydrodynamics and regional climate dynamics over the Great Lakes region. The seasonal and interannual variability of the regional climate, lake circulation, thermal structure, and ice

cover of each lake are examined, along with estimates of surface heat and moisture fluxes.

The remaining parts of this paper are organized as follows. In sections 2 and 3, we describe the configuration of the coupled lake–atmosphere model, the design of the numerical simulations, and the model validation data used in this study. In section 4, we discuss the modeling results in comparison with a wide array of in situ and satellite datasets. The results of two extreme events (the 2012 "big heat" and 2014 "big chill") are examined in section 5, followed by discussion and conclusions in sections 6 and 7.

2. Models and data

To the best of our knowledge, this is the first documentation of a two-way coupled, 3D regional climate modeling system for the Great Lakes, including a 3D hydrodynamic model of lake circulation, thermal structure, and ice dynamics. We refer to the new modeling system as the Coupled 3D Great Lakes–Atmosphere Regional Model (C-3D–GLARM) to distinguish it from previous models that use 1D, 2D, and/or uncoupled (or one-way coupled) numerical modeling approaches. Hereinafter, C-3D-GLARM is abbreviated as GLARM for brevity.

a. Regional climate model

The latest (fourth) version of the International Centre for Theoretical Physics (ICTP) Regional Climate Model (RegCM4) is used to simulate land and atmospheric processes (Giorgi et al. 2012). RegCM4 is a 3D, hydrostatic, compressible, primitive equation, σ-coordinate regional climate model based on the hydrostatic version of the Fifth-generation Pennsylvania State University–National Center for Atmospheric Research (PSU–NCAR) Mesoscale Model (MM5) (Grell et al. 1994; Pal et al. 2000). The model physics are similar to those of RegCM3 and are described in detail in Pal et al. (2007), Steiner et al. (2009), and Wang et al. (2016). It adopts the Community Climate Model version 3 (CCM3)-based package for atmospheric radiative transfer computations (Kiehl et al. 1996) and nonlocal formulation of the planetary boundary layer from Holtslag et al. (1990). The large-scale cloud and precipitation schemes are resolved by the explicit cloud/ precipitation scheme of Pal et al. (2000), and the unresolvable precipitation processes (cumulus convection) are represented using the Grell parameterization (Grell 1993; Grell et al. 1994). The model version used in this study is based on Wang et al. (2016), with carbon–nitrogen dynamics (CN) and dynamic vegetation (DV) components turned off, and surface physics calculations are performed using the Community Land Model, version 4 (CLM4), to represent soil–vegetation hydrological processes of the

land surface. Surface fluxes over water (e.g., oceans and lakes) are handled by Zeng's bulk aerodynamic ocean flux parameterization scheme (Zeng et al. 1998).

RegCM4, by default, can be coupled to the 1D, energy-balanced, diffusion–convection lake model described by Hostetler et al. (1993), as well as the one-layer ice model from Patterson and Hamblin (1988) at each model lake grid cell. In this configuration, the 1D models are distributed spatially across a 2D domain, and the energy is transferred between layers by eddy and molecular diffusion and by vertical convective mixing. This coupled RegCM4 1D lake–atmosphere modeling system has been applied to the Great Lakes in a number of previous studies (Notaro et al. 2013; Bennington et al. 2014; Notaro et al. 2015). In particular, Bennington et al. (2014) demonstrated in great detail the performance of the coupled RegCM4 1D lake simulation for the Great Lakes, including challenges and failures with the default model, improvements in the modified version, and the overall fundamental limitations of such a model.

Our RCM modeling domain covers not only the Great Lakes region but also the majority of North America. There are 350×360 horizontal grid points at 18-km grid spacing (Fig. 1) and 18 vertical sigma layers. It is worth noting that most previous RCM studies for the Great Lakes have been isolated to the immediate surrounding region, which can constrain the system to the large-scale, driving AOGCM dynamics. These studies have also been performed at a coarser resolution (e.g., 25–60 km), which can leave many finer-scale processes unresolved. The lateral atmospheric boundary conditions for our regional climate modeling system are provided by ERA-Interim climate reanalysis data from the European Centre for Medium-Range Weather Forecasts (ECMWF). Lateral boundary conditions include 6-hourly surface pressure and wind components, air temperature, and mixing ratio at all vertical model levels.

b. Hydrodynamic model

The Great Lakes hydrodynamic model used in this study is based on the Finite Volume Community Ocean Model (FVCOM) (Chen et al. 2006), a free-surface, primitive equation hydrodynamic model that solves the momentum, continuity, temperature, salinity (often not used for the Great Lakes), and density equations and is closed physically and mathematically using turbulence closure submodels. FVCOM is solved numerically using the finite-volume method in the integral form of the primitive equations over an unstructured triangular grid mesh and vertical sigma layers. This approach combines the best features of an unstructured grid for ideal geometric fitting and the flexibility of local mesh refinement (similar to finite-element methods), as well as numerical
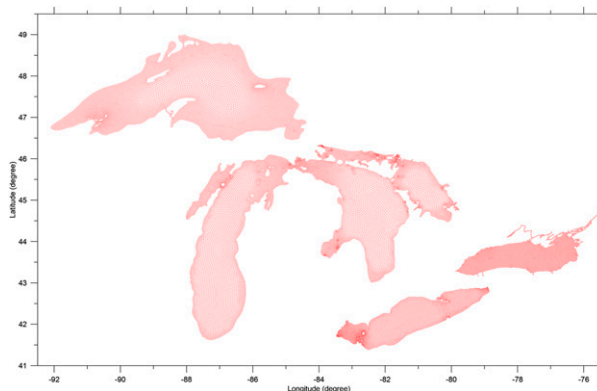

FIG. 2. Unstructured triangular mesh used in the Great Lakes 3D hydrodynamic model.

efficiency and code simplicity (similar to finite-difference methods). FVCOM has been widely implemented in coastal ocean applications (Xue et al. 2011, 2012), as well as the Great Lakes (Shore 2009; Anderson and Schwab 2013; Xue et al. 2015). Other hydrodynamic models have also been used for the Great Lakes (e.g., Schwab and Bedford 1994; Beletsky et al. 2006; Wang et al. 2010; Huang et al. 2010; Fujisaki et al. 2012), but all of these models were developed in one-way or uncoupled modes.

The horizontal resolution of the model triangular grids varies from ~1–2 km near the coast to ~2–4 km in the offshore regions of the lakes (Fig. 2). The model is configured with 40 sigma layers to provide a vertical resolution of <1 m for nearshore waters and ~2–5 m in most of the offshore regions of the lakes. The Mellor–Yamada level-2.5 (MY25) turbulence closure model (Mellor and Yamada 1982) is used for simulating vertical mixing processes, which includes a set of prognostic equations for turbulent kinetic energy and a length scale–related parameter to calculate eddy viscosities and vertical diffusivities. The horizontal diffusivity is calculated using the Smagorinsky numerical formulation (Smagorinsky 1963), determined by the horizontal velocity shear as well as the model grid resolution. We note here that although the five Great Lakes are geographically distinct, Lakes Michigan and Huron are hydraulically connected, so the system can often be treated as four enclosed basins when hydrodynamics and regional climate are of interest.

c. Ice model

To simulate ice–water interaction processes, we adapted the Los Alamos Community Ice Code (CICE) into an unstructured-grid, finite-volume version within the FVCOM framework (Gao et al. 2011). CICE uses four layers of ice and one layer of snow and is governed by energy-conserving thermodynamics (Maykut and Untersteiner 1971; Bitz and Lipscomb 1999),

elastic–viscous–plastic ice momentum equations (Lipscomb and Hunke 2004), and energy-based ridging schemes of Thorndike et al. (1975) and Lipscomb et al. (2007), with ice strength parameterizations given by Rothrock (1975). Ice cover in the Great Lakes typically lasts 3–5 months every year and is confined within the closed basins. Thus, we developed a simplified and much more computationally efficient version of CICE as an energy-conserving thermodynamic model of ice. Its governing equation is well described by Bitz and Lipscomb (1999), and we adapted the ice fraction calculation at each individual model cell by calculating the evolution of the ice thickness distribution in time and space through thermodynamic growth and melting.

The simplified ice model is very computationally efficient, allowing us to conduct coupled atmosphere–hydrodynamic ice simulations that span more than a decade in length. Even so, it is still a more sophisticated model than the default ice model in RegCM4 since it allows for ice fraction calculation at each model cell based on the ice thickness distribution (ITD) function. More importantly, the model is employed in the FVCOM model grid at a resolution of 1–2 km, which is a much higher resolution than the ice model employed in RegCM4 (18-km grid spacing).

d. Data for model validation

To validate the atmospheric components of the GLARM modeling system, we focus on the climatic trends, spatial patterns, and interannual variability in surface air temperature and precipitation, both at the synoptic scale of North America and the regional scale of the Great Lakes. Model results are evaluated against station-based observational datasets over North America, namely the global land-station-based 0.5° resolution datasets produced by the Climate Research Unit (CRU, version 3.0) for the period 1982–2013 (Harris et al. 2014). Over the Great Lakes, we evaluate the model-simulated precipitation and evaporation fields against estimates from the Great Lakes Hydro-Climate Dashboard (GLHCD), which are products based on a combination of models and observations (Gronewold et al. 2013; Clites et al. 2014a; Hunter et al. 2015).

For comparisons of LSTs, we evaluate the model results against the Great Lakes Surface Environmental Analysis (GLSEA2) (available from https://coastwatch.glerl.noaa. gov/glsea/glsea.html). To date, GLSEA2 serves as the best resource to examine spatial and temporal variability of surface water temperature. Through the NOAA CoastWatch program, GLSEA2 provides daily digital maps of the Great Lakes LST. The LST data are stored as a 1024×1024 pixel map, available in Portable Network Graphics (PNG), ASCII, and netCDF formats, suitable for visualization and further manipulation with readily available software. The data are derived from NOAA Advanced Very High Resolution Radiometer (AVHRR) satellite imagery and are updated daily with information from the cloud-free portions of the previous day's satellite imagery. To generate continuous evolution of the LST, a smoothing algorithm is applied to the previous day's available map when no imagery is available, as described by Schwab et al (1992). In addition, direct in situ measurements of LST from the National Data Buoy Center (NDBC) (available from http://www.ndbc.noaa.gov/) are analyzed over the five Great Lakes to assist in model evaluation. Moored water temperature data collected at the western basin of Lake Superior for the year 2011, and maintained by University of Minnesota, Duluth (Titze and Austin 2014), are also used to evaluate model simulations of subsurface water temperature for both coupled and uncoupled 3D circulation models. The mooring is located close to NDBC buoy station 45006 at 47.335°N, 89.793°W, at a local water depth of 183 m.

Ice cover data over the Great Lakes are collected by the Canadian Ice Service and U.S. National Ice Center (available from http://www.natice.noaa.gov/products/great_lakes. html) at a temporal resolution of 3–7 days. The observations are constructed using various imagery sources, with pixel resolutions down to 50 m. The data also include necessary value-added interpretations of these imagery sources to properly identify the extent of the ice edge contours. Data used in the present study are linearly interpolated to daily time scales, and comparisons are performed to evaluate model simulations of ice coverage and duration.

GLARM-simulated precipitation and evaporation over the Great Lakes are evaluated against lakewide average estimates from the GLHCD dataset (only lakewide average monthly estimates are available), which assimilates nearshore, overlake, and watershed-based hydrometeorological measurements into model simulations of the major components of the water budget for the Great Lakes basin (Hunter et al. 2015). The GLHCD estimates overlake precipitation via spatial interpolation using a modified version of Thiessen weighting and data from stations that are located near shore or on islands and offshore lighthouses (Hunter et al. 2015). GLHCD monthly overlake evaporation estimates for each lake are obtained from daily simulations using NOAA/GLERL's 1D Large Lake Thermodynamics Model (LLTM), forced by aggregated nearshore and offshore hydrometeorological measurements (Hunter et al. 2015).

3. Design of numerical simulations

RegCM4 simulations were conducted over North America for approximately three decades, from 1982 to

TABLE 2. Summary of numerical model simulations.

Model configuration	Simulation period (spinup excluded)	LST boundary condition	Meteorological forcing of lake models	Purpose
RegCM4 stand-alone	20 yr (1983–2002)	Prescribed by daily OISST	—	Part of RCM validation
GLARM	12 yr (2003–14)	Simulated by the coupled 3D circulation model	Simulated by the coupled RCM with 3D hydrodynamics	Part of RCM validation; GLARM validation
RegCM4 coupled with 1D lake	4 yr (2011–14)	Simulated by the coupled 1D lake model	Simulated by the coupled RCM with 1D thermal dynamics	Intercomparison of RCM coupled with 1D vs 3D lake model
3D lake circulation model (FVCOM) stand-alone	2 yr (2010–11)	—	Simulated by RegCM4 coupled with 1D lake model	Intercomparison of coupled vs uncoupled 3D circulation model (forecast scenario)
3D lake circulation model (FVCOM) stand-alone	2 yr (2010–11)	—	Simulated by RegCM4 with LST prescribed by GLSEA	Intercomparison of coupled vs uncoupled 3D circulation model (hindcast scenario)

2014 (Table 2). We first ran RegCM4 as a stand-alone, uncoupled model for the first two decades (1982–2001), initialized at 1 January 1982 using the first year as spinup. During the period of stand-alone simulation (1982–2001), the SST of the ocean and LST of the lakes were prescribed by weekly 0.5° resolution NOAA daily Optimum Interpolation SST (OISST) (Reynolds et al. 2007). RegCM4 was then coupled with the hydrodynamic and ice models for the remaining 13 years (2002–14), using a 1-yr spinup (2002) for the hydrodynamic ice model. During the two-way coupled simulation period (2002–14), the two model components ran simultaneously, with coupled information exchange between RegCM4 and FVCOM at 3-h intervals. We note that tests with a higher coupling frequency showed no significant improvement against more computational time. In the two-way coupled framework, the LST fields and ice coverage are dynamically calculated by the 3D hydrodynamic model and ice model and provided to RegCM4 as overlake surface boundary conditions. In turn, the surface forcing fields required by the hydrodynamic and ice models are dynamically calculated and provided by the coupled atmospheric model component. These fields include wind velocity, precipitation, relative humidity, cloud cover, and incoming shortwave and longwave radiation. Instantaneous estimates of latent and sensible heat flux and upward longwave radiation are made within FVCOM at each time step using simulated LSTs with the COARE, version 2.6, bulk algorithm (Fairall et al. 1996).

Although the MY25 submodel is currently the most robust commonly used turbulence closure scheme in Great Lakes 3D hydrodynamic models, the accurate simulation of vertical mixing processes in water is still a challenging prospect in the hydrodynamic modeling community. Overmixing with the MY25 submodel during the fall season has occasionally been found to occur in the Great Lakes (Xue et al. 2015). Hence, a nudging scheme is applied during November and December to constrain deep-water temperatures (>100-m depth) to 4°C or cooler (the temperature of maximum density for freshwater), in case overmixing occurs during fall turnover.

There are several practical reasons why the above model configuration is used in order to optimize the computational efforts:

1) For evaluating RegCM4's performance in simulating long-term climate trends and variability over North America, the full simulation time spanning more than three decades (1982–2014) is clearly needed to provide an objective assessment.

2) Because of computational loads, the GLARM simulation is performed only for 2003–14 (i.e., 12 yr). This is sufficient to appropriately evaluate the simulation
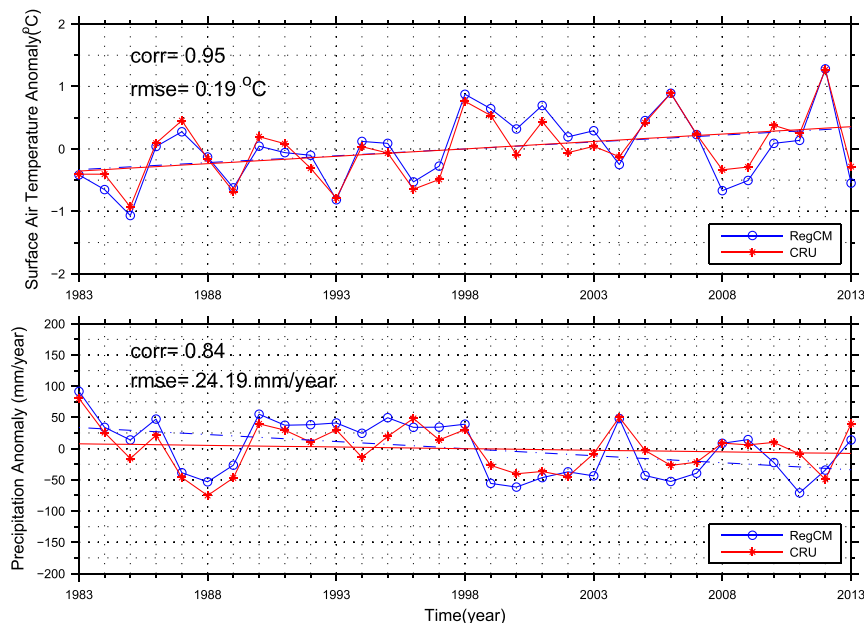
FIG. 3. (top) Annual temperature anomalies and (bottom) precipitation anomalies over North America for the period 1983–2013 from the model simulation and CRU observations.

of Great Lakes hydrodynamic and ice thermodynamics in the new regional climate modeling system, particularly given the large interannual variability during the 2012–14 period.

3) As dimictic lakes, the memory of initial conditions for the Great Lakes should generally be less than one year; hence, a 1-yr spinup (2002) of the hydrodynamic model is appropriate.

4) High-resolution ice atlas data (for model evaluation) are available from 2002 onward.

To assess the improvements of GLARM over other model configurations (1D coupling and uncoupled 3D circulation models), we conducted three additional experiments: one simulation with RegCM4 coupled with the 1D lake model and two simulations with the 3D FVCOM model in a stand-alone, uncoupled configuration with RegCM4. Additional details regarding the various simulation experiments are provided in Table 2.

4. Results

a. Simulated air temperature and precipitation

We begin by evaluating the modeled surface climatology of air temperature and precipitation to assess the degree to which the model can capture regional climate trends and variability, not only for the Great Lakes region but also across North America. The comparison helps to provide confidence in the performance of the RCM, which is a prerequisite to ensure the accurate

representation of regional climate interactions with the Great Lakes hydrodynamic and ice models.

As a measure of how well the model reproduces the observed interannual variability and long-term trends in domain-averaged North American air temperature and precipitation, the observed and simulated annual anomalies for both variables over the period 1982–2013 are compared (Fig. 3). The model accurately captures both the interannual variability and climatic warming trend of surface air temperature over the past three decades. The simulated and observed temperature anomalies are highly correlated, with a correlation coefficient of 0.95 and a root-mean-square error (RMSE) of 0.19°C. The simulated long-term warming trend of 0.24°C decade^{-1} compares very well with the observed trend of 0.25°C decade^{-1}, indicating that the model captures the climatic trend as well as the interannual variability. In terms of annual precipitation, the model similarly produces robust results in comparison with the CRU data, with a high correlation coefficient of 0.84 and a low RMSE of 24 mm (compared to an annual mean precipitation of 748 mm). Aside from a few exceptions (e.g., 2011), most of the wet years (e.g., 1983, 1990, 1993, and 2004) and dry years (e.g., 1988, 2002, and 2012) are well captured by the model.

Figure 4 presents a comparison of the simulated and observed spatial distribution of the climatological annual mean surface air temperature and precipitation. The model reproduces the observed spatial patterns in air temperature reasonably well, including large temperature gradients over the Rocky Mountains in the western United States
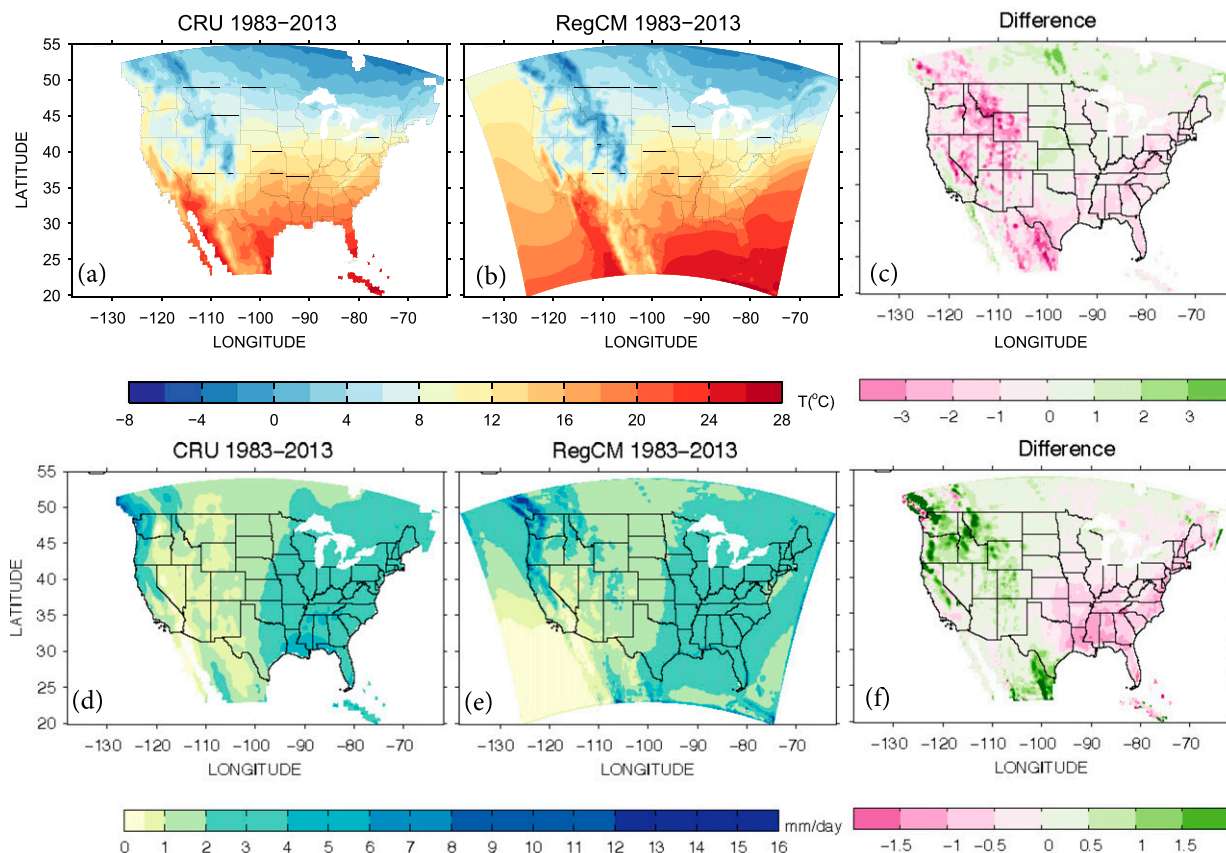
FIG. 4. Model–data comparison showing the climatology of (a)–(c) surface air temperature and (d)–(f) precipitation over North America (1983–2013). (left) CRU observations, (center) model simulation, and (right) difference (model minus observations).

and a meander of warmer temperature intrusions in the southern and central United States (Figs. 4a,b). The pattern correlation between the modeled and observed climatology of surface air temperature is 0.83. Differences between the modeled and observed temperature maps (Fig. 4c) show close agreement over the majority of North America, with errors of ~1°C throughout the Great Plains, Midwest, Southwest, Southeast, and Northeast regions. Larger errors of up to 3°C are present over the Rocky Mountain region, which is likely due to the complex topography and model-resolution issues. Over the Great Lakes region, the modeled annual and seasonal (Fig. S1 in the supplemental material) air temperature climatology agrees very well with observations, with biases of less than 1°C during all seasons except winter (Fig. S1). This exception is associated with a warm bias over the northern boundary of the model domain during winter (DJF), which affects the water temperature and ice cover simulation (section 4b) of Lake Superior, particularly the northern portion. A direct comparison of the spatial pattern of air temperature between the RegCM4 boundary input files generated from ERA-40 and the CRU observations suggests that the warm bias in

the northern boundary is most likely inherited from the driving ERA-40 product (not shown).

In terms of annual precipitation, both the spatial pattern and magnitude of the simulated precipitation rate are consistent with observations (Figs. 4d,e), with a pattern correlation of 0.88. This includes the general pattern of low precipitation to the west of the Missouri River, higher precipitation to the east, and a narrow band of high precipitation along the Pacific Northwest. The difference map (Fig. 4f) reveals some wet biases in regions of steep topography and a general dry bias in the southeastern United States, but the Great Lakes region shows generally good model–observation agreement, with most errors in seasonal precipitation being generally less than 0.5–1.0 mm day^{-1} aside from a few locations in lake-effect precipitation belts (Fig. S2 in the supplemental material).

b. Great Lakes surface water temperature

As mentioned previously, our primary research goal in this study is to improve the simulation of large lakes in regional climate modeling. Toward this end, we compare the model-simulated and observed LST for each of the
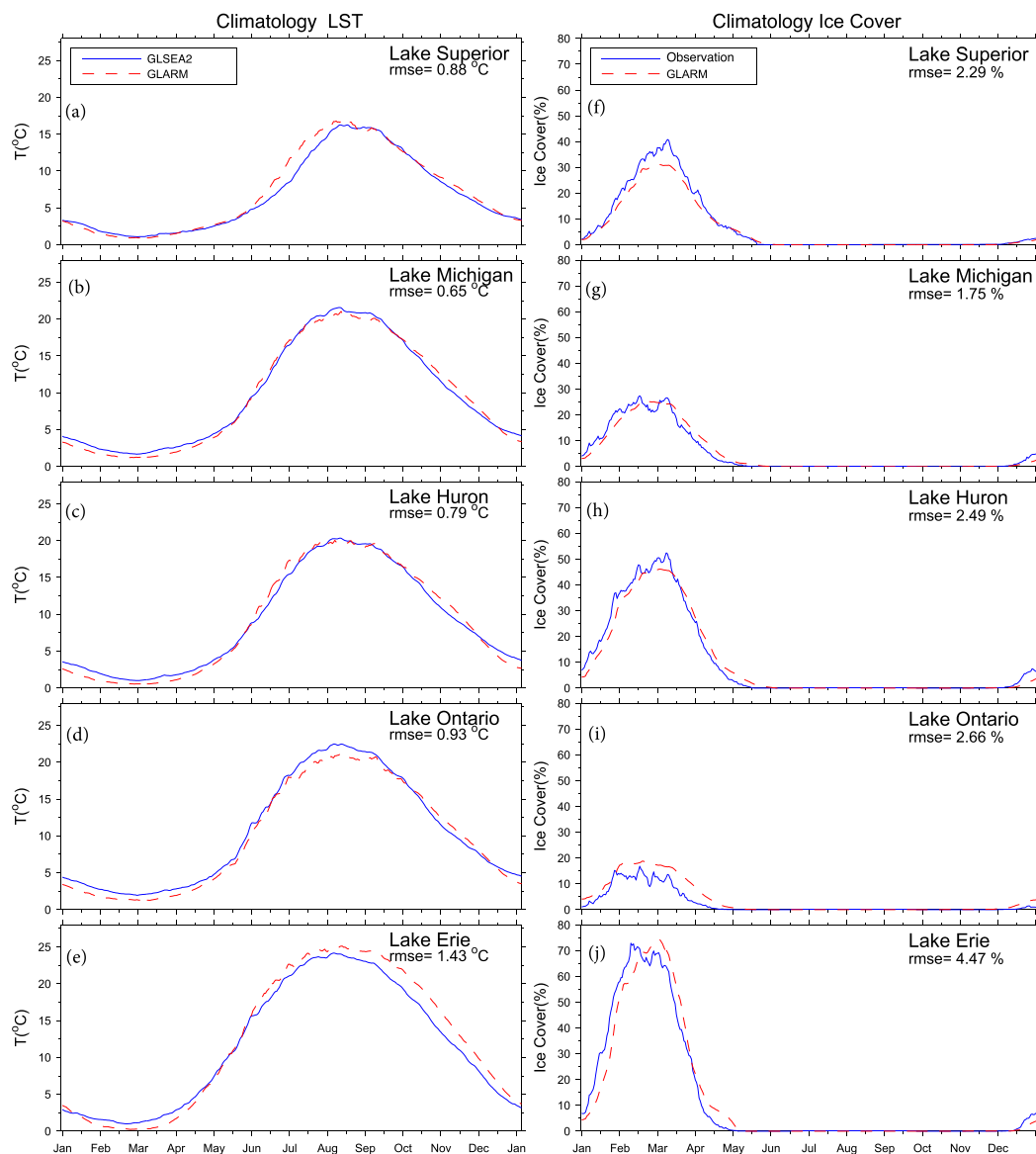
FIG. 5. Climatology (2003–14) of daily (a)–(e) LST and (f)–(j) ice coverage from the GLARM simulation (red dashed lines) and observations (blue lines; LST from GLSEA2 and ice cover from the National Ice Center).

Great Lakes over the period 2003–14 (Figs. 5 and 6). At the climatological mean seasonal time scale, the modeled LST agrees well with observations in each lake (Figs. 5a–e). For Lake Superior, the model shows a close agreement with GLSEA2 with an RMSE of 0.88°C. The most noticeable bias occurs during summer (June–August). For Lake Michigan and Lake Huron, the difference in the mean seasonal cycle of LST between the model and GLSEA2 are 0.65° and 0.79°C, respectively, without a particular bias in specific seasons. For Lake Ontario, there is a slight underestimate of summer LST, and the RMSE is 0.93°C. Relatively larger bias occurs in Lake Erie, where the model shows an overestimate from June to December,

with an RMSE of 1.43°C. Reasons for such bias are unclear and would require additional experiments to determine.

In addition to comparing the mean seasonal climatology of LST with observations for our model assessment, we also present a model–data comparison of LST and ice cover anomalies (deviations from the mean seasonal climatology) for 12 consecutive years (2003–14) (Figs. 6 and 9). This provides a more rigorous comparison since it requires the model to reproduce both the climatological mean seasonal cycle, as well as monthly to interannual variability. The GLARM modeling system accurately captures the interannual variability of LST in all five lakes, with much of the LST variability
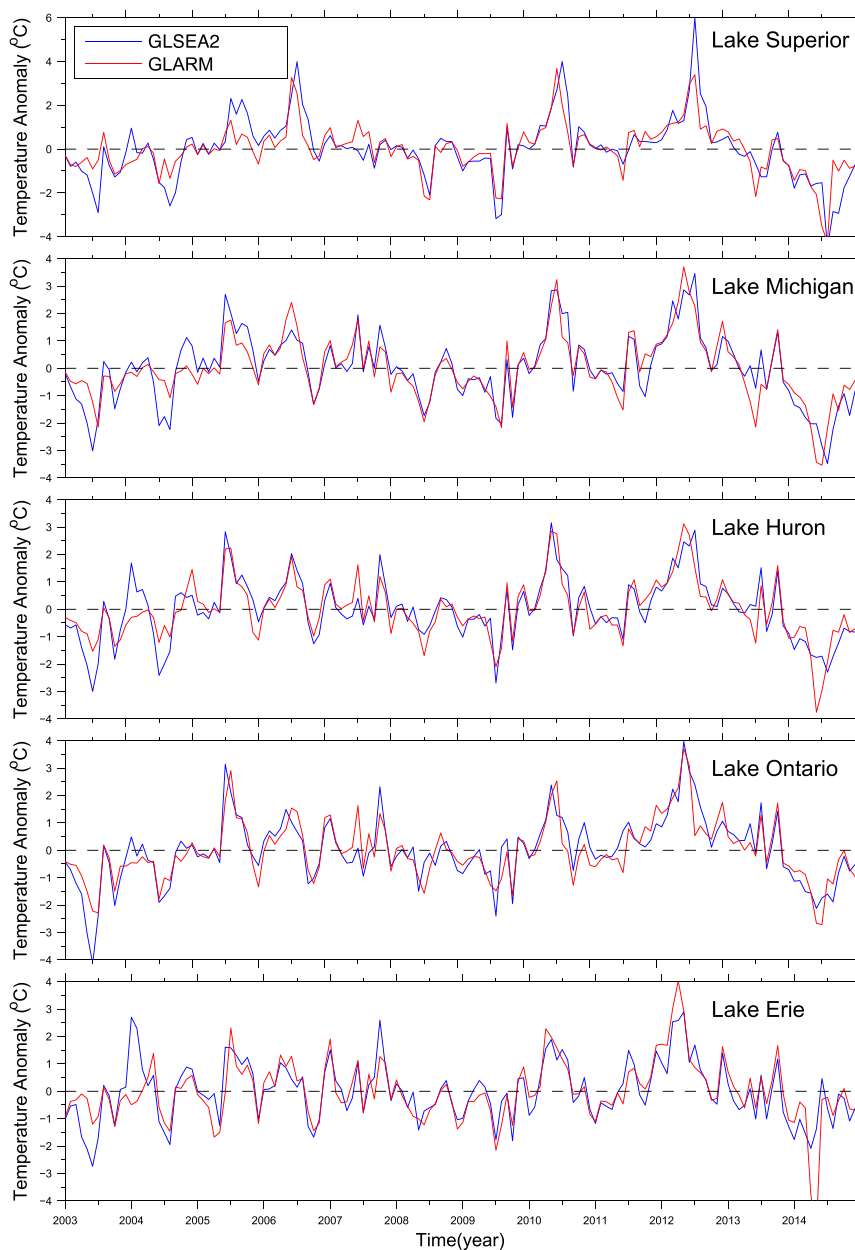
FIG. 6. Time series of lake-average LST anomalies (monthly value minus long-term monthly mean; 2003–14) as simulated by GLARM (red) and compared with GLSEA2 observations (blue).

being significantly influenced by each lake's depth and geographic characteristics. Although the shallower lakes exhibit larger seasonal variability in climatological LST (e.g., ~25°C for Lake Erie compared to ~18°C for Lake Superior; Fig. 5), all five of the lakes exhibit similarly strong interannual variability in LST, with a range of ±4°C (Fig. 6). Such variability can become accentuated during extreme climatic events, such as the cold winter of 2013/14, which led to significantly reduced summer LSTs on Lake Superior during 2014 (up to 4°C below its

climatology value) because of significant delays in summer stratification.

In addition to comparing the lakewide average LST with the satellite-derived GLSEA2 data, we also assessed GLARM performance against spatially distributed, in situ LST measurements at all nine NDBC buoys on the five Great Lakes, which are located well offshore but in a variety of different water depths. For comparison, we also ran RegCM4 with the default 1D lake model. For brevity, we only show results for the last four years of the
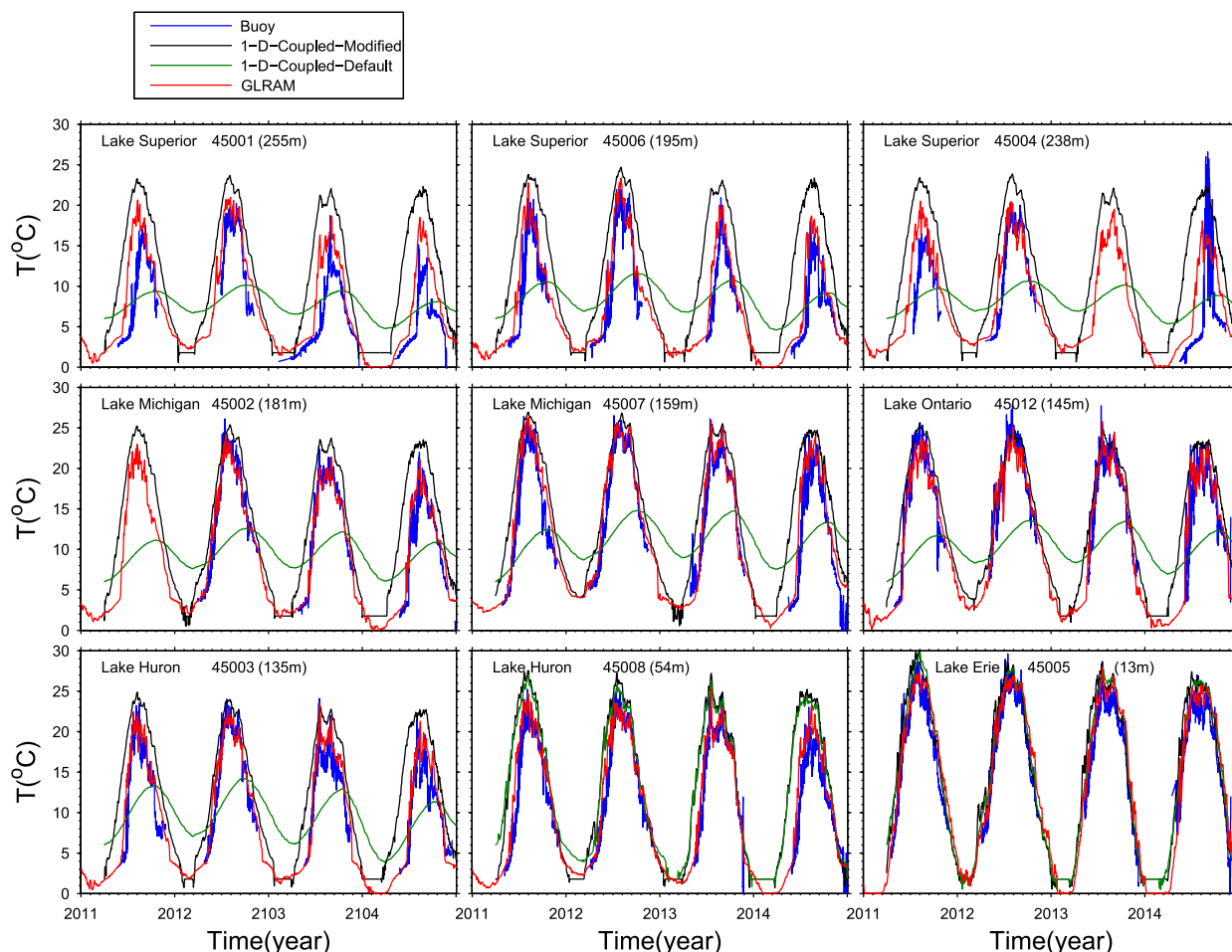
FIG. 7. Time series of surface water temperature simulated by GLARM (red), RegCM4 coupled with 1D default (green) and modified (black) lake models in comparison with in situ measurements at nine NDBC buoy stations (blue; see Fig. 1 for buoy locations) for 2011–14.

simulation (Fig. 7), which include a very warm year (2012) and very cold year (2014). The 1D lake model distributed in the 2D domain only captures the seasonal variability of LST at two shallow sites—one in western Lake Erie (45005; 13 m) and the other in southern Lake Huron (45008; 54 m). Otherwise, the default 1D model (green line) fails to resolve the seasonality of LST at the other seven stations with greater water depth. The 1D model results (black line) are largely improved after we modified the convective mixing algorithm for buoyancy-induced instability, but they still show considerably large biases in comparison to the observations (blue line). Similarly poor results from the default 1D lake model coupled in RegCM4 have been shown before in Fig. 3 of Bennington et al. (2014), who provided a detailed assessment and further refinement of the 1D lake model simulation when coupled with RegCM4. In contrast, the new results from GLARM show excellent agreement with each of the nine in situ buoy measurements on the Great Lakes, regardless of water depth.

Because of the immense surface area and abruptly changing bathymetry, Great Lakes LSTs vary significantly across each lake, particularly during the summertime. Figure 8 shows the spatial pattern of the seasonal climatology of LST from GLARM and GLSEA2 data. During the springtime (Figs. 8a,b), the spatial variability of LST has just begun to develop within each lake, and the temperature pattern reflects the impacts of variations in water depth and latitude, resulting in earlier springtime warming in the southern lakes and shallower water. In summer, strong thermal gradients continue to be evident across latitude and varying water depths (e.g., coastal slope zones; Figs. 8c,d). The spatial patterns of modeled summer LST are particularly well captured for Lakes Michigan, Huron, and Ontario, while the model slightly overestimates LST in midlake portions of Lake Superior and southwestern portions of Lake Erie.

During autumn, LST decreases to ~7°C in Lake Superior and ~12°C in Lake Erie because of reductions in
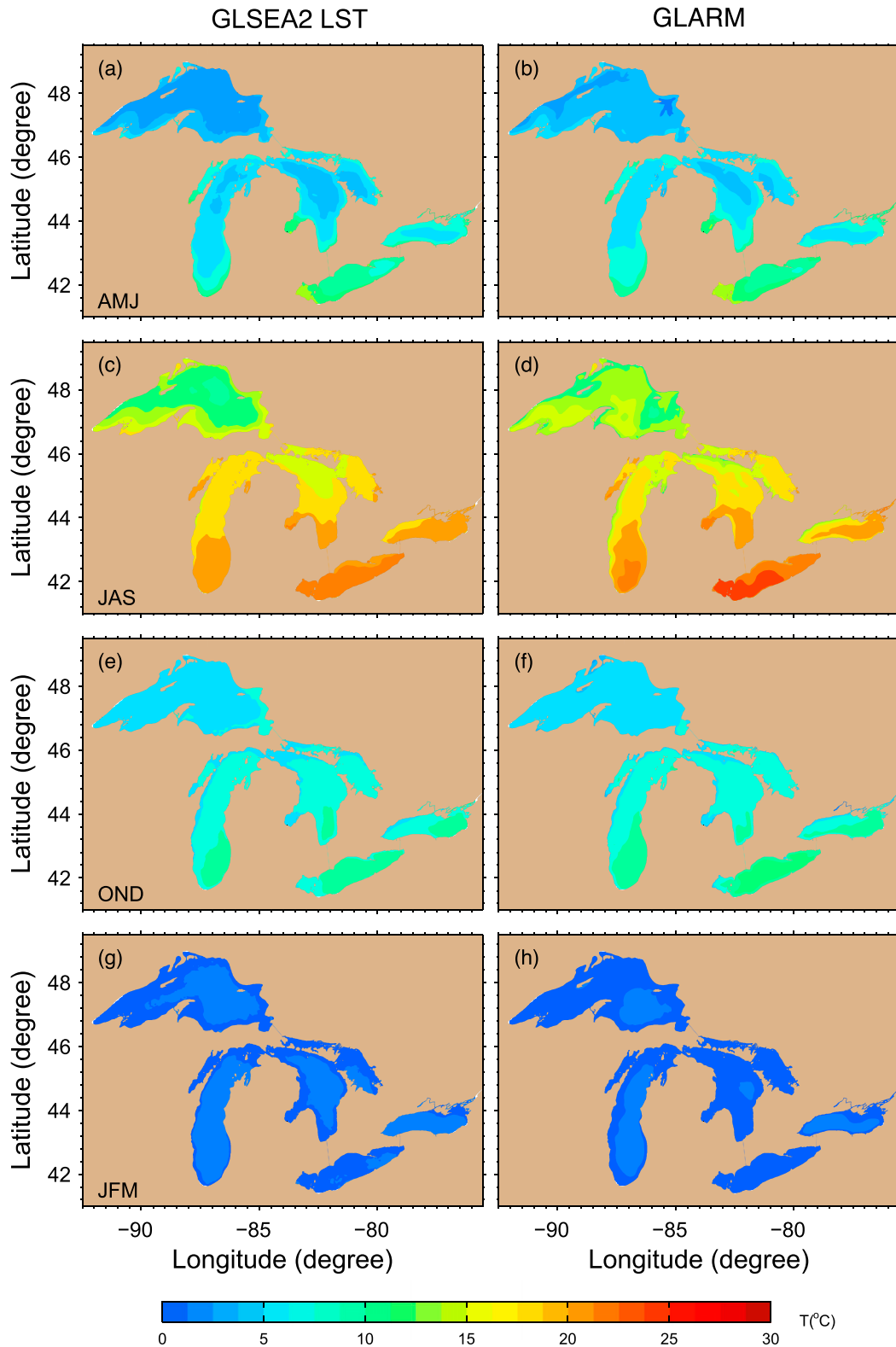
FIG. 8. Model–data comparison of the LST seasonal climatology (2003–14) during (a),(b) spring [April–June (AMJ)], (c),(d) summer [July–September (JAS)], (e),(f) fall [October–December (OND)], and (g),(h) winter [January–March (JFM)]. GLSEA2 observations are shown in (a),(c),(e), and (g); GLARM simulation is shown in (b),(d),(f), and (h).
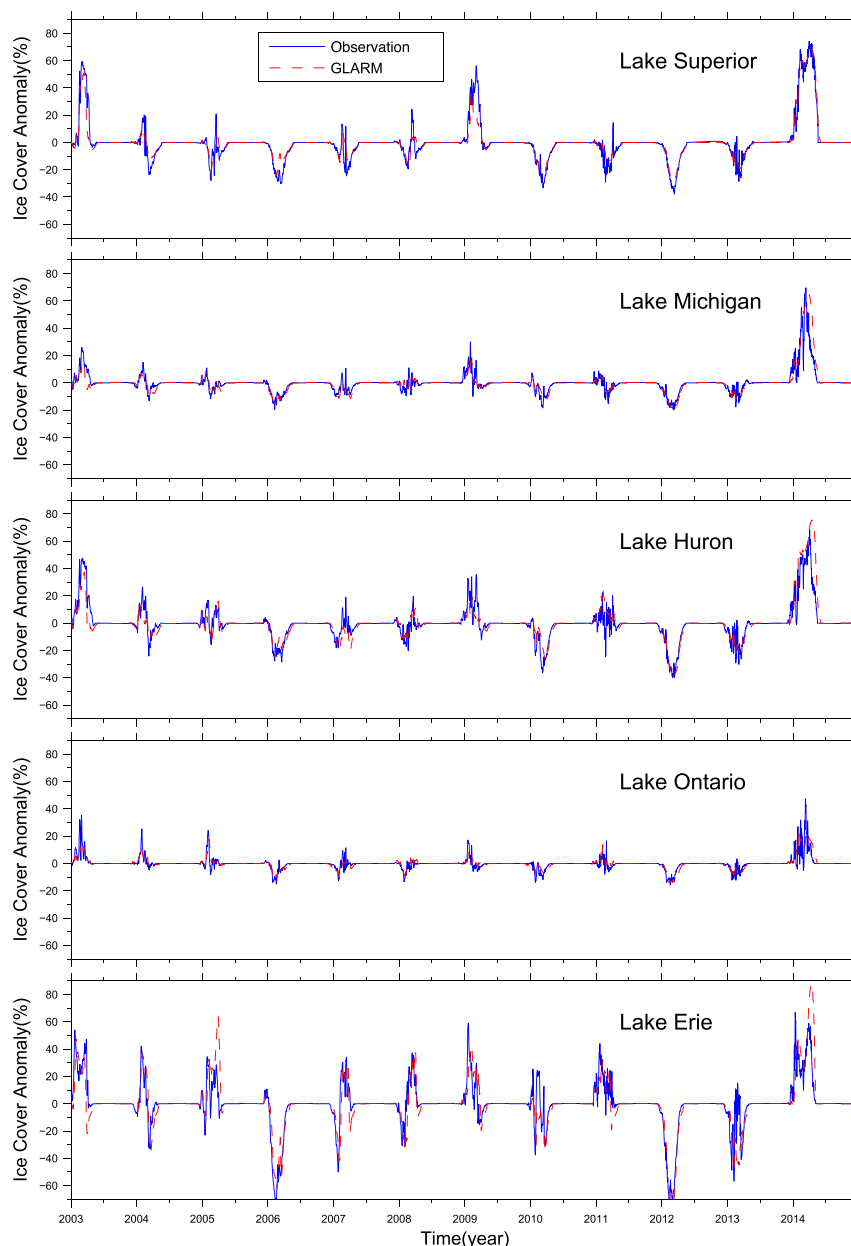
FIG. 9. Time series of lake-average ice cover anomalies (daily value minus long-term daily mean; 2003–14) as simulated by GLARM (red) and compared with observations (blue) from the National Ice Center.

net radiation and increases in latent and sensible heat flux associated with stronger winds and frequent passages of cold, dry air (Blanken et al. 2011; Xue et al. 2015). The spatial pattern of LST becomes fairly homogenous within each lake, except for Lakes Michigan and Huron because of its extensive orientation in the meridional direction (Figs. 8e,f). Surface cooling continues through winter (Figs. 8g,h), accompanied by rapid ice formation in the nearshore regions (discussed in the next section) and relatively lower ice coverage in

midlake, due to both larger heat content in deep water and strong winds in the open water that can retard ice formation (Assel 1990; Wang et al. 2012).

c. Ice simulation for the Great Lakes

In the Great Lakes, ice cover plays an important role in shaping the lakes' energy and water balance by affecting net radiation, evaporation (latent heat), and sensible heat flux. Simulation of ice cover in the Great Lakes has long been a challenge, and there have been

few models (1D or 3D) that are able to address the issue satisfactorily (Dupont et al. 2012). On one hand, GLARM captures reasonably well the seasonal and interannual variability in ice cover, as well as the differences among lakes (Figs. 5, 9, and S4 in the supplemental material). On the other hand, peak areal ice coverage in Lake Superior tends to be underestimated (Fig. 5f), likely because of the aforementioned warm bias in winter air temperature over the Lake Superior region in RegCM4 (Fig. S1). Both model and observations indicate that Lake Huron and Lake Michigan have peak ice coverage of ~50% and ~25%, respectively, in the seasonal climatology (Figs. 5g,h), with ice typically diminishing below ~10% by late April. Lake Ontario (Fig. 5i) shows the least ice cover among the five lakes—with a typical year having only 15%–20% maximum areal ice coverage—primarily because Lake Ontario is the second deepest of the five Great Lakes (by mean depth), while also being in a warmer, southeastern location that is generally downwind of the other lakes. As the shallowest lake, Lake Erie (Fig. 5j) develops the highest ice coverage (with mean peak coverage around 70%–75%).

GLARM also captures the interannual variability of ice cover reasonably well, showing large variability in all five lakes (Fig. 9). For example, the anomalies in peak ice coverage for Lake Superior are ~50%–75% above normal during cold winters (2003, 2009, and 2014), while ice coverage may be ~20%–30% below normal in warm years (2006, 2010, and 2012). Similar patterns are observed in other lakes except Lake Ontario, which shows lower variability, similar to its lower mean values. Lake Erie often shows much larger intraseasonal variability, such as double-peak patterns during cold winters (2003 and 2014); abruptly changing above- and below-normal ice cover in 2004, 2007, and 2008; and exceptional low-ice years during 2006 and 2012. Interannual variability of ice cover on Lake Huron is also quite large, with peak values that range from 60% above normal to 40% below normal, while the largest ice cover anomalies on Lake Michigan are usually no more than 30% above normal, with 2014 (>90%) being the primary exception. Abnormally low ice cover during the warm years of 2006 and 2012 is also well captured by the model across all the lakes (Figs. 9 and S4).

In addition to areal ice coverage, the duration of winter ice cover (from ice onset to ice offset, which is defined with a threshold of 10% ice coverage within an observation pixel or a model grid) is another key characteristic that is important to examine for the Great Lakes. The climatology of observed ice duration from the National Ice Center for the period 2003–14 is compared with the GLARM simulation in Fig. 10. The

simulated spatial distribution of ice duration agrees with observations in general, but some discrepancies exist in various locations, particularly Lake Superior. Aside from the north shore of Minnesota, the model tends to underestimate ice duration over the majority of Lake Superior, as would be expected from the underestimated ice coverage (Fig. 5) and aforementioned warm bias in winter air temperature. The model does, however, capture the general pattern of longer ice duration in the shallow, nearshore regions and shorter ice duration in the deeper, offshore locations—not only for Lake Superior but the other four lakes as well. This includes a number of shallow regions in Lakes Michigan and Huron with longer ice duration, such as Green Bay, Georgian Bay, the Straits of Mackinac, and the southern shore of Lake Huron. The climatological pattern of ice duration in Lake Ontario is also well captured (particularly the strong gradients in the northeastern portion of the lake), as is the much higher ice duration in Lake Erie and especially in the shallow, western basin (~70–90 days).

d. Overlake evaporation and precipitation

Overlake evaporation and precipitation are important components of the energy and water budgets of the Great Lakes, yet very few overlake hydrometeorological measurements are available (Blanken et al. 2011; Spence et al. 2013). While this makes it extremely difficult to derive measurement-based spatial patterns of overlake precipitation and evaporation, it also highlights the value of integrating observations and RCM modeling systems such as GLARM for estimating Great Lakes surface energy and water fluxes (Hunter et al. 2015).

Figure 11 presents a comparison of the simulated and observed 12-yr monthly climatology of mean overlake precipitation and evaporation. Results from GLARM and GLHCD show similar modeled and observed seasonality, with some variations among lakes that reflect differences in atmospheric and hydrodynamic conditions. For example, the lowest evaporation rates generally occur in early to late spring, when water temperatures are still cold, but the air is becoming warmer and more humid (Lenters 2004). This minimum evaporation occurs in April for Lake Erie, May for Lakes Michigan, Huron, and Ontario, and June for Lake Superior. The earlier minimum for Lake Erie occurs as a result of the fact that the lake warms and stratifies much faster because of its shallow depth and southern location, which allows the lake–air moisture gradient to evolve faster and in earlier seasons than the other lakes. Similarly, the highest evaporation rates occur earlier for Lake Erie (October) and later for Lake Superior (December–January), which reflects both the larger
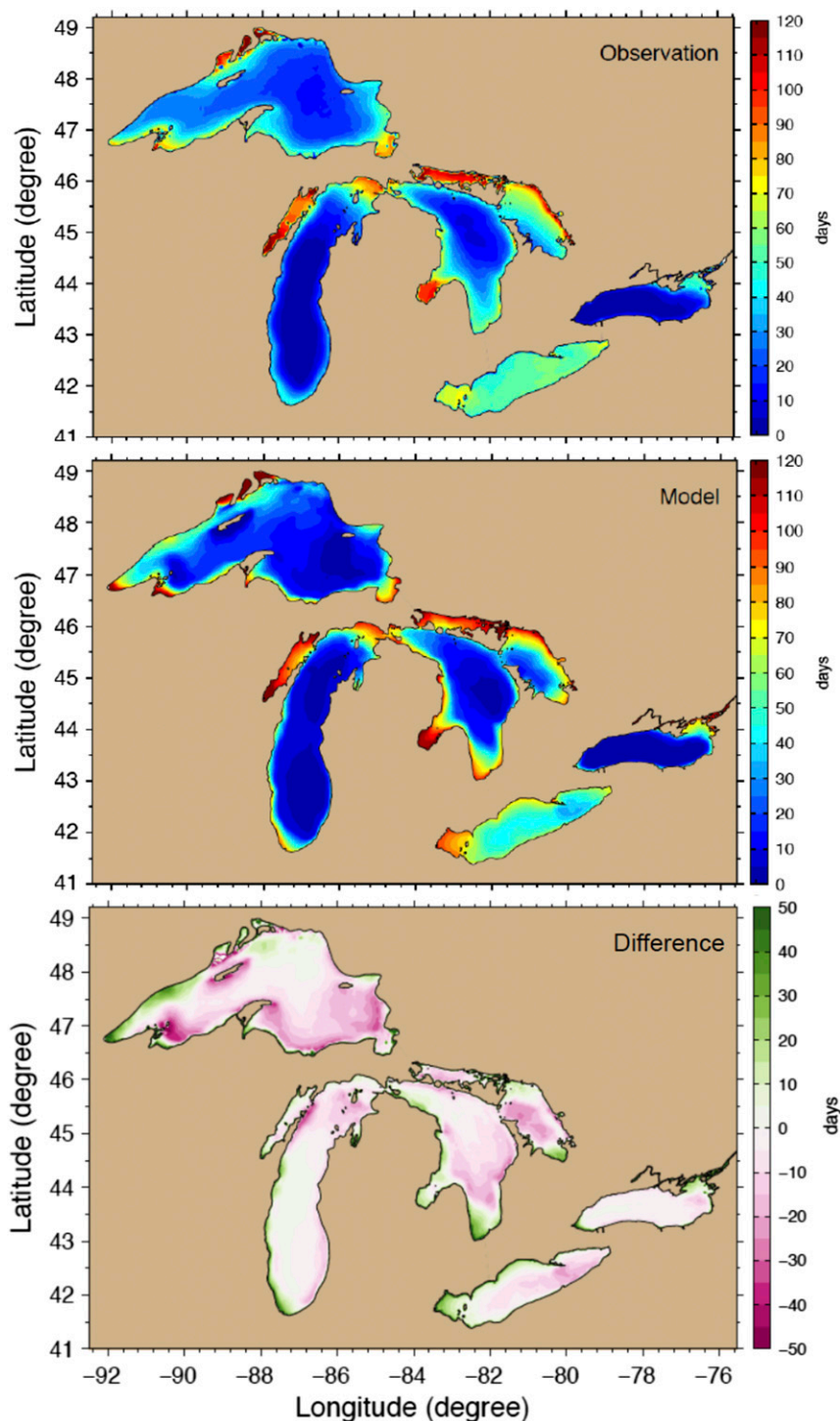
FIG. 10. Climatology of observed ice duration on the Great Lakes (days) from (top) the National Ice Center and (middle) the GLARM simulation for the period 2003–14. (bottom) The difference (model minus observed).

thermal inertia of Lake Superior and the more extensive ice coverage on Lake Erie. Autumn Lake Erie evaporation rates in GLARM are considerably lower than those from GLHCD LLTM, but it is suspected that this reflects evaporation rate overestimates in the LLTM simulation, which are unrealistically higher than even the highest rates on Lake Superior. Observed and simulated overlake precipitation generally display good agreement for all four
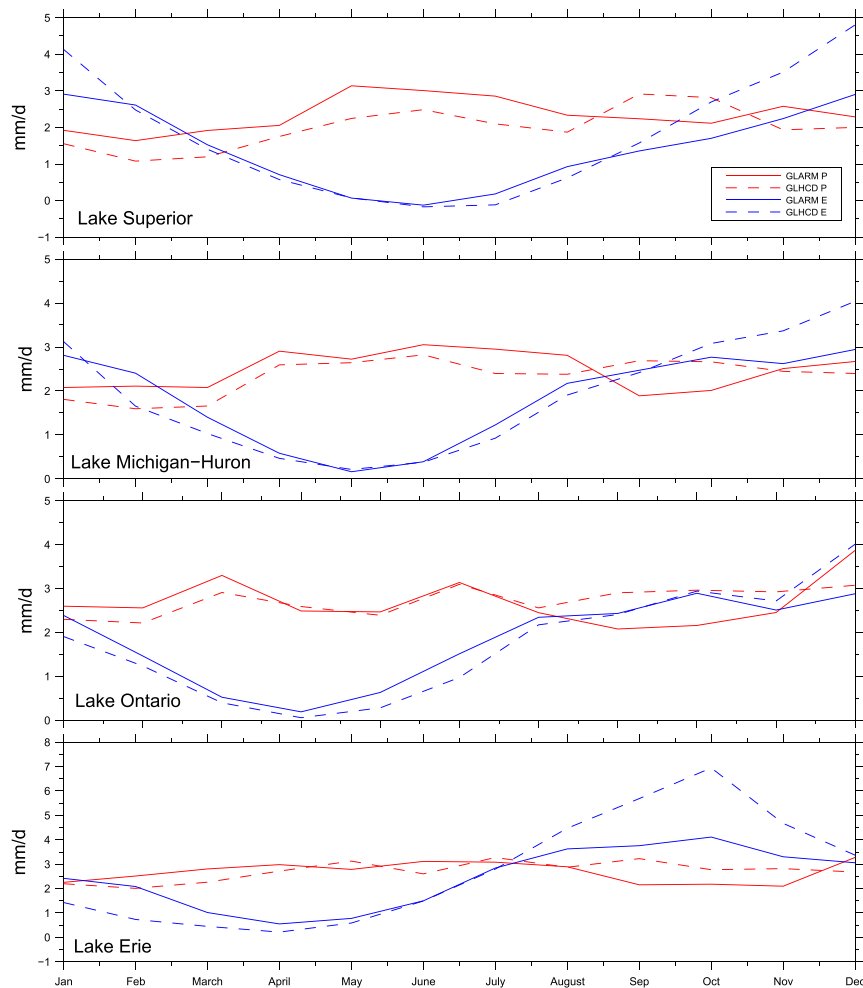
FIG. 11. Seasonal climatology of monthly mean overlake precipitation (red) and evaporation rate (blue) from GLHCD observations and GLARM simulation results (2003–14).

lakes, including a slight tendency for higher precipitation rates in late spring and early summer (e.g., Lakes Superior and Michigan–Huron). Precipitation estimates from GLARM during the autumn seasons are generally lower than the GLHCD, suggesting either a bias in the GLHCD spatial interpolation of land-based stations or an underestimate of modeled precipitation.

5. Extreme climatic events: The "big heat" (2012) and "big chill" (2014)

During the winter of 2011/12, the United States experienced the fourth warmest winter on record in more than a century (NCEI 2013). Located near the warming center, the Great Lakes had the lowest ice coverage on record since the 1960s (Figs. 9 and S4), resulting in an exceptionally early onset of stratification, a longer period of stratification, and a deeper thermocline. Figure 12

(left) demonstrates the evolution of lake thermal structure during 2012 for each of the five Great Lakes, as simulated by the GLARM modeling system. Separated by only one intervening year, the Great Lakes region then experienced an extremely cold winter in 2013/14, caused by anomalous intrusions of Arctic air and high-amplitude wave patterns in the jet stream (commonly referred to in the media as the polar vortex). As a result, the Great Lakes experienced an extended period of ice coverage—even into the month of June for Lake Superior—which was followed by a significantly delayed and shorter period of stratification, along with a shallower thermocline (Fig. 12, right).

These recent extreme climatic events have raised challenging questions for the regional climate modeling community, as it is becoming apparent that strong interannual climatic variability is inherent to the Great Lakes system (Van Cleave et al. 2014; Gronewold et al.
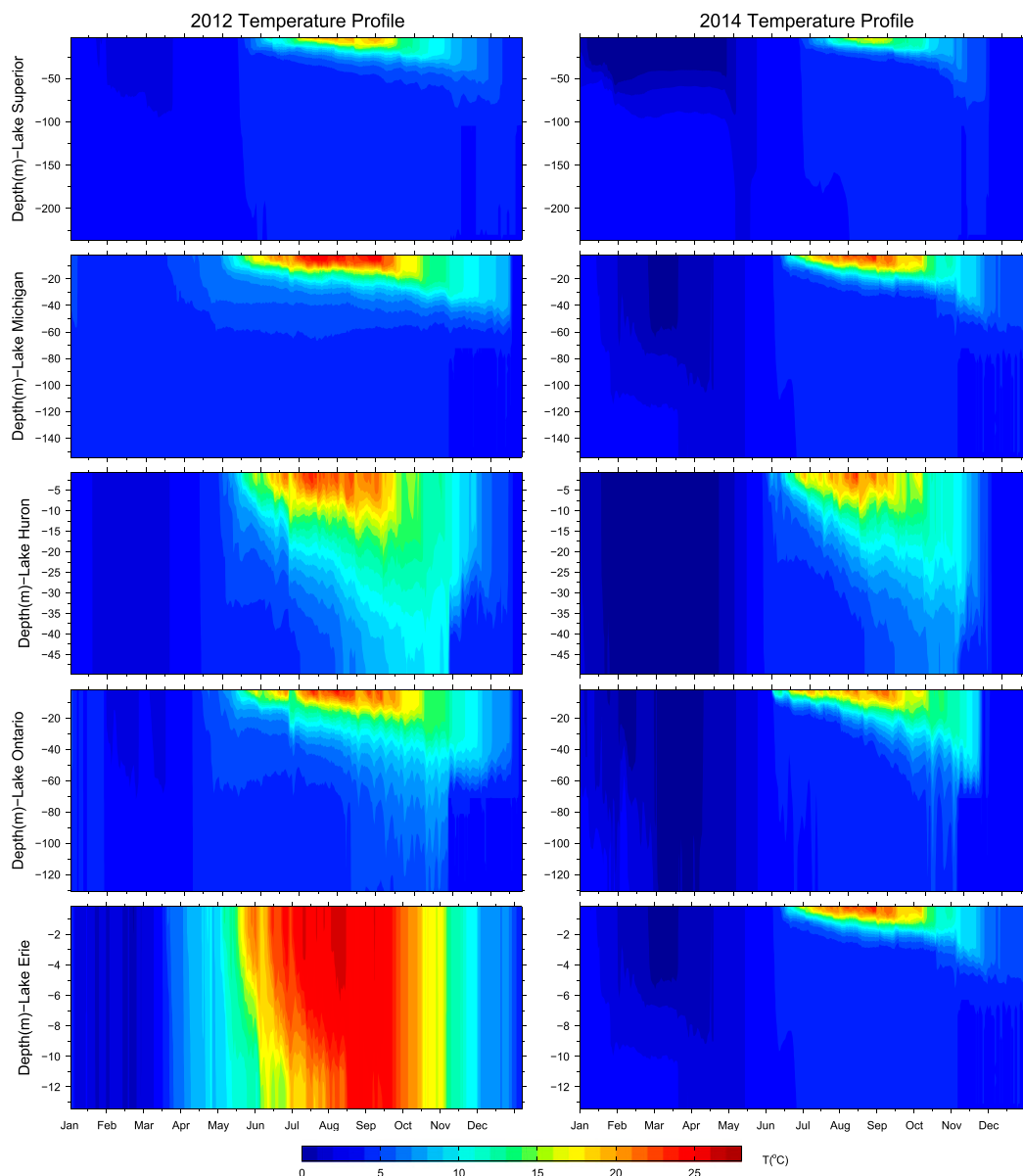
FIG. 12. Simulated Great Lakes water temperature profiles from the GLARM model at various buoy locations ([Fig. 1]) on Lake Superior (45001), Lake Michigan (45007), Lake Huron (45008), Lake Ontario (45012), and Lake Erie (45007) during the (left) "big heat" of 2012 and (right) "big chill" of 2014.

2015). Thus, it is important to determine not only the extent to which Great Lakes climatic trends (and impacts) can be predicted but also how well we can predict extreme fluctuations.

6. Discussion

a. Necessity of resolving 3D hydrodynamics

In many large-lake systems, including the Great Lakes, hydrodynamic processes that control thermal structure are far more complicated than simple 1D vertical mixing. The dynamic regimes in the Great Lakes vary appreciably with changes in water depth and can be divided into offshore water, the coastal boundary layer, and nearshore regions, similar to coastal oceans. Each region is characterized by a different momentum balance that essentially determines the multiscaled flow structures in the Great Lakes. In the open water, the momentum balance is primarily between the Coriolis force and barotropic (wind driven) and baroclinic (thermal driven) pressure gradient forces, while in the coastal boundary layer the
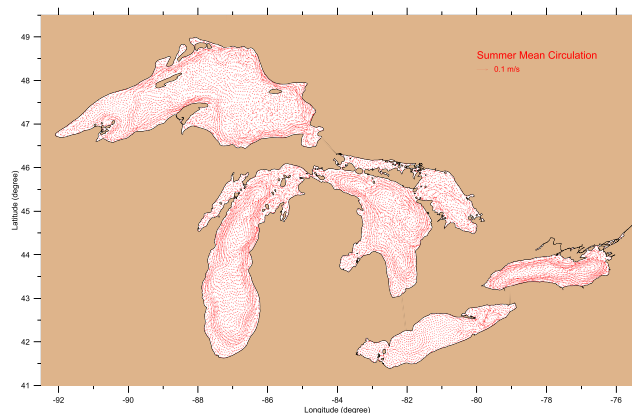
FIG. 13. JAS-mean circulation patterns on the Great Lakes (upper 20 m) as simulated by the GLARM model for the period 2003–14.

bottom and lateral frictional forces play an important role in the momentum balance.

As demonstrated in Fig. 13, the mean horizontal flow structure in the near-surface layer of the Great Lakes features multigyre circulations and strong coastal jet currents with strong spatial variability. Beletsky et al. (1999) and Rao and Schwab (2007) give excellent summaries on these flow patterns and related physical processes. Furthermore, short-term flow conditions and thermal structures during episodic events, such as storms, further complicate the system, as transient surface velocities can reach >10–20 cm s^{-1}, with spatial temperature gradients exceeding 0.01°C m^{-1} in the thermal bar region. In addition, the vertical flow structures that directly impact and respond to mixing processes can also be extremely complex, such as double-cell secondary circulation at thermal fronts (Chen et al. 2001) or two-layer baroclinic flows like those that occur in the Straits of Mackinac during the summer stratified season (Anderson and Schwab 2016, manuscript submitted to *J. Geophys. Res. Oceans*). Also, surface inertia–gravity (Poincaré) waves, Kelvin waves, and topographic waves can induce mixing across thermal gradients.

As mixing processes are closely associated with water velocity shear in both the horizontal and vertical dimensions (Smagorinsky 1963; Mellor and Yamada 1982), such flow-dependent mixing processes are unresolvable in a 1D lake model, where mixing coefficients are typically determined only as a function of wind. Because of the different spatial scales of atmospheric and hydrodynamic processes and the complexities of hydrodynamic conditions, the wind-based mixing coefficients are oversimplified, with much less accuracy in resolving spatial variability in mixing processes. Therefore, although 1D lake models may work well in small

and shallow lakes, where hydrodynamic processes are relatively homogeneous, large-lake systems almost always require substantial empirical calibration of eddy diffusivity with a factor that could range from 10^2 to 10^5 at various water depths to compensate for not explicitly simulating 3D mixing processes that influence thermal transfer (Gu et al. 2015) or use a "virtual bottom cutoff," often at 50 m, to tackle this issue (Gula and Peltier 2012; Subin et al. 2012).

Advective transport of heat is another equally important process for large lakes that is unresolved in 1D lake models. During the stratified season, significant wind events create upwelling and downwelling of the thermocline because of Ekman transport. These circulation patterns can create regions that transport significant heat. The wind-driven and density-driven circulations also transport and redistribute heat within the lake. The resulting thermal gradients in turn support and sustain circulation patterns and waves. These processes are completely neglected in 1D vertical thermal balance models.

It is evidently important to use 3D, primitive equation, turbulent closure circulation models to represent the hydrodynamics (rather than 1D lake models) across a wide range of water depths in all five lakes, especially for simulating impacts on lake thermal structure and subsequent lake–atmosphere interactions.

b. Inclusion of coupled lake–air dynamics in hydrodynamic simulations

Although 3D circulation models have been fairly widely applied in "stand alone" fashion for a variety of Great Lakes and oceanographic applications, two major challenges are commonly recognized by the hydrodynamic modeling community: 1) the uncertainty of surface forcing representations and 2) the failure to
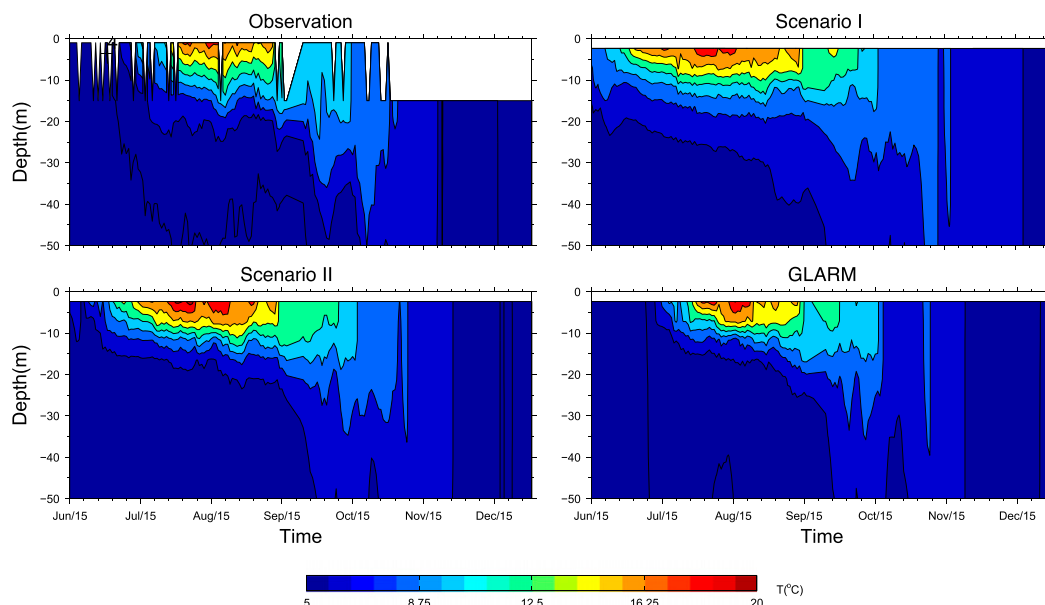
FIG. 14. Model–data comparison of time evolution of the lake subsurface thermal structure in the western basin of Lake Superior for 2011 (see section 2 for mooring data description).

effectively resolve air–sea feedback processes. A dynamic representation of meteorological conditions has been suggested to reduce surface forcing uncertainty in hydrodynamic modeling (Xue et al. 2015), which also suggests that resolving water–air feedback processes should improve model performance.

To examine how much model improvement in the current study is due to the utilization of a two-way coupled modeling approach, we conducted a "model assessment simulation" to compare GLARM with an uncoupled 3D hydrodynamic model simulation. We note that we retained all the model configurations (i.e., model parameters and temporal and spatial resolution) to be exactly the same as those in the original GLARM simulation.

To demonstrate the importance of two-way coupling for Great Lakes hydrodynamic simulations, two scenarios are considered. In both scenarios, we use the same regional climate model and 3D circulation model (FVCOM) but without the GLARM framework (i.e., uncoupled). The first scenario (scenario I) is intended for hydrodynamic forecasting/prediction and does not include observed LSTs to drive the RCM. Rather, the RegCM4 is first coupled with the default 1D lake model to generate the surface forcing field that is then used to drive the 3D lake circulation model. The second scenario (scenario II) is a hydrodynamic hindcast simulation wherein the RegCM4 was run with observed lake surface boundary conditions from the GLSEA2 daily LST, and the output was then used to drive the 3D

FVCOM model. In scenario II, the hydrodynamic simulation is expected to be better than scenario I since the output from the RegCM4 simulation has eliminated LST-induced errors that may be present in scenario I. Both cases were hot-started from coupled simulation results ending on 31 December 2009 and continue through 2011 (2-yr simulation). We examine the models' performance in simulating the vertical structure of water temperature in Lake Superior at the western basin offshore buoy location and in comparison with observations and the GLARM simulation.

Figure 14 presents a model–data comparison of the time evolution of the subsurface thermal structure in the western basin of Lake Superior. The results demonstrate improvements in the model simulation as a result of resolving lake–air feedbacks using a two-way coupled model. Scenario I (Fig. 14, top right) shows the poorest simulation results: namely, that the water stratifies much earlier than suggested by the observations, and the mixing depth tends to deepen too rapidly from summer into autumn, with warm water lingering in the subsurface until mid-December (i.e., later than observed). In comparison, results from scenario II (Fig. 14, bottom left) show some improvement, with more accurate onset of stratification and mixed-layer depth. The overpredicted warm water from mid-November to December has also been corrected to a large degree. The most accurate simulation (Fig. 14, bottom right) is provided by the GLARM model, showing a simulated thermal structure that agrees well with observations. The model

improves the accuracy of the onset of stratification in mid-July. The warm bias in the upper 20 m from September to October is corrected, and the cooling of water after November is also more accurately simulated. The only result that worsens slightly is the underestimate of near-surface temperature during the short period from mid-October to early November. These comparisons not only validate the GLARM simulation of subsurface water temperature but also demonstrate the importance of using a two-way coupled model approach for 3D hydrodynamic simulation of the Great Lakes, particularly as a tool for future prediction.

Another example that supports the integrated modeling approach is the reasonably accurate simulation of ice cover and duration despite the use of a relatively simple ice thermodynamic model in the integrated modeling system. These results suggest that proper simulation of complex ice structure on the Great Lakes is more strongly linked to the high resolution, accuracy, and interactions between atmospheric conditions (e.g., surface heat fluxes and winds) and hydrodynamic conditions (e.g., surface water temperature and currents) than to the complexity of the ice model itself. In other words, without an accurate representation of both the atmospheric and hydrodynamic components, it is implausible to deliver an accurate ice simulation regardless of the level of sophistication in the existing ice model.

The underlying mechanisms of how the representations of water–air interactions influence both hydrodynamic and atmospheric model performances vary significantly depending on characteristics of the regional climate (Wei et al. 2014; Turuncoglu et al. 2013; Xue et al. 2014, 2015). Zhang et al. (1995), Terray et al. (2012), and Masson et al. (2012) suggest that short-term (e.g., intradaily, daily) variability of surface water temperature could impact the regional climate by cascading short-term fluctuation into the larger-scale motion; Xue et al. (2014) and Xue and Eltahir (2015) demonstrate that simulations were improved through direct local-scale air–sea feedbacks that primarily controlled vertical thermal dynamic processes. Zhang et al. (1995) show that the improvement could be a combined influence of local and large-scale processes. For large lakes, the local-scale feedbacks that control overlake heat flux components or heat redistribution are likely to play a dominant role (Song et al. 2004; Xue et al. 2015) rather than feedbacks that modify large-scale atmospheric circulation. This is also evident in our results through the comparison of the heat budgets simulated by the GLARM and the RCM-coupled default 1D lake models (next section) since differences are primarily shown in variables that are directly affected by surface water temperature.

c. Impact of 3D hydrodynamic modeling on atmospheric variables

Comparing differences between the surface heat and water budgets simulated by the GLARM system and the RCM-coupled default 1D lake models (Figs. S5–S9 and Table S1 in the supplemental material), the results show that the most substantial differences are primarily for variables that are directly affected by surface water temperature, including evaporation, sensible heat flux, and upward longwave radiation. Although further improvements can certainly be made to the 1D models (Bennington et al. 2014), the unresolved hydrodynamics in the RCM-coupled 1D model are found to cause large biases in the LST simulation (e.g., Fig. 6), which consequently causes an excessive bias in annual evaporation amounts (e.g., an average difference of ~0.3 m across the five Great Lakes, Table S1). The corresponding overestimate of annual latent heat flux is ~25 W m^{-2}, compared to the estimates from GLARM. Sensible heat flux and upward longwave radiation are also overestimated in the 1D model by an average of 13 and 5 W m^{-2}, respectively. Noticeable but smaller differences of 0.17 mm day^{-1} are found in the simulation of precipitation, which is likely due to the fact that both large-scale precipitation, which is less impacted by change in LST, and local convective precipitation, which is more sensitive to local conditions, contribute to the total precipitation. There are no significant changes in other atmospheric variables such as solar radiation and cloud coverage when RegCM4 is coupled with the 1D lake model. We note that the above comparisons were made using seasonal and annual time scales and basin-averaged values. It is anticipated that there should be more noticeable impacts in the atmospheric variables at shorter time scales and finer spatial scales, although such analyses are currently beyond the scope of this study.

7. Summary and conclusions

In this study, we developed a regional lake–climate modeling system (GLARM) composed of an RCM coupled with a 3D hydrodynamic lake and ice model, with a focus on the long-standing issue of simulating large, deep lakes within a climate modeling setting. In our two-way coupled modeling system, the water temperature, lake ice, and atmospheric surface conditions are simulated simultaneously with different model components in GLARM, and these variables are allowed to freely interact among each other. Results show that the simulations of the Great Lakes thermal structure, surface fluxes, and ice are improved significantly compared to previous studies that have utilized simpler modeling systems. Characteristics of the atmosphere

and the lake thermal structure, hydrodynamics, and ice are all well captured by GLARM, indicating the unique capability of each modeling component (as well as the integrated model) for accurately representing the various components of the regional lake–climate system.

Despite these initial successes of the GLARM modeling system, there is still plenty of room for future improvement. While the ice model adequately simulates the thermodynamics of ice formation on the Great Lakes, horizontal transport and mechanical redistribution of ice certainly play important roles in large lakes such as the Great Lakes. This is even more crucial if the simulation is focused at short time scales (e.g., hourly, daily, or weekly). Future work will incorporate an ice dynamics simulation into the coupled modeling system once the existing numerical code of ice dynamics is upgraded to make it more computationally efficient. Model improvements can also be made in terms of the parameterization of lake–air heat, momentum, and moisture fluxes. Our ongoing research into different bulk parameterizations suggests that GLARM currently produces reasonable estimates of latent and sensible flux but that these estimates may exhibit higher uncertainty during late autumn and winter (often when the fluxes are largest). Additional corrections, therefore, may provide further improvements in the simulation of ice cover, water temperature, and hydrodynamics not only during cold months but in other seasons as well, particularly for the deeper lakes. In addition, by converting runoff information from RegCM4 into river inflow in FVCOM and building an interconnected five Great Lakes hydrodynamic model, GLARM will be able to provide a complete estimate of the surface water cycle for the Great Lakes basin.

REFERENCES

Anderson, E. J., and D. J. Schwab, 2013: Predicting the oscillating bi-directional exchange flow in the Straits of Mackinac. *J. Great Lakes Res.*, **39**, 663–671, doi:10.1016/j.jglr.2013.09.001.

Assel, A. A., 1990: An ice-cover climatology for Lake Erie and Lake Superior for the winter seasons 1897–1898 to 1982–1983. *Int. J. Climatol.*, **10**, 731–748, doi:10.1002/joc.3370100707.

Austin, J. A., and S. M. Colman, 2007: Lake Superior summer water temperatures are increasing more rapidly than regional air temperatures: A positive ice-albedo feedback. *Geophys. Res. Lett.*, **34**, L06604, doi:10.1029/2006GL029021.

Beletsky, D., J. H. Saylor, and D. J. Schwab, 1999: Mean circulation in the Great Lakes. *J. Great Lakes Res.*, **25**, 78–93, doi:10.1016/S0380-1330(99)70718-5.

——, D. Schwab, and M. McCormick, 2006: Modeling the 1998–2003 summer circulation and thermal structure in Lake Michigan. *J. Geophys. Res.*, **111**, C10010, doi:10.1029/2005JC003222.

Bennington, V., M. Notaro, and K. D. Holman, 2014: Improving climate sensitivity of deep lakes within a regional climate model and its impact on simulated climate. *J. Climate*, **27**, 2886–2911, doi:10.1175/JCLI-D-13-00110.1.

Bitz, C. M., and W. H. Lipscomb, 1999: An energy-conserving thermodynamic model of sea ice. *J. Geophys. Res.*, **104**, 15 669–15 677, doi:10.1029/1999JC900100.

Blanken, P. D., C. Spence, N. Hedstrom, and J. D. Lenters, 2011: Evaporation from Lake Superior: 1. Physical controls and processes. *J. Great Lakes Res.*, **37**, 707–716, doi:10.1016/j.jglr.2011.08.009.

Chen, C., J. Zhu, E. Ralph, S. A. Green, J. W. Budd, and F. Y. Zhang, 2001: Prognostic modeling studies of the Keweenaw Current in Lake Superior. Part I: Formation and evolution. *J. Phys. Oceanogr.*, **31**, 379–395, doi:10.1175/1520-0485(2001)031<0379:PMSOTK>2.0.CO;2.

——, R. C. Beardsley, and G. Cowles, 2006: An unstructured grid, finite-volume coastal ocean model (FVCOM) system. *Oceanography*, **19** (1), 78–89, doi:10.5670/oceanog.2006.92.

Clites, A. H., J. P. Smith, T. S. Hunter, and A. D. Gronewold, 2014a: Visualizing relationships between hydrology, climate, and water level fluctuations on Earth's largest system of lakes. *J. Great Lakes Res.*, **40**, 807–811, doi:10.1016/j.jglr.2014.05.014.

——, J. Wang, K. B. Campbell, A. D. Gronewold, R. A. Assel, X. Bai, and G. A. Leshkevich, 2014b: Cold water and high ice cover on Great Lakes in spring 2014. *Eos, Trans. Amer. Geophys. Union*, **95**, 305–306, doi:10.1002/2014EO340001.

Dupont, F., P. Chittibabu, V. Fortin, Y. R. Rao, and Y. Lu, 2012: Assessment of a NEMO-based hydrodynamic modelling system for the Great Lakes. *Water Qual. Res. J. Canada*, **47**, 198–214, doi:10.2166/wqrjc.2012.014.

Fairall, C. W., E. F. Bradley, D. P. Rogers, J. B. Edson, and G. S. Young, 1996: Bulk parameterization of air–sea fluxes for Tropical Ocean–Global Atmosphere Coupled–Ocean Atmosphere Response Experiment. *J. Geophys. Res.*, **101**, 3747–3764, doi:10.1029/95JC03205.

Feser, F., B. Rockel, H. von Storch, J. Winterfeldt, and M. Zahn, 2011: Regional climate models add value to global model data: A review and selected examples. *Bull. Amer. Meteor. Soc.*, **92**, 1181–1192, doi:10.1175/2011BAMS3061.1.

Fujisaki, A., J. Wang, H. Hu, D. J. Schwab, N. Hawley, and Y. R. Rao, 2012: A modeling study of ice–water processes for Lake Erie applying coupled ice-circulation models. *J. Great Lakes Res.*, **38**, 585–599, doi:10.1016/j.jglr.2012.09.021.

Gao, G., C. Chen, J. Qi, and R. C. Beardsley, 2011: An unstructured-grid, finite-volume sea ice model: Development, validation, and application. *J. Geophys. Res.*, **116**, C00D04, doi:10.1029/2010JC006688.

Giorgi, F., 2006: Regional climate modeling: Status and perspectives. *J. Phys. IV*, **139**, 101–118, doi:10.1051/jp4:2006139008.

——, and Coauthors, 2012: RegCM4: Model description and preliminary tests over multiple CORDEX domains. *Climate Res.*, **52**, 7–29, doi:10.3354/cr01018.

Grell, G. A., 1993: Prognostic evaluation of assumptions used by cumulus parameterizations. *Mon. Wea. Rev.*, **121**, 764–787, doi:10.1175/1520-0493(1993)121<0764:PEOAUB>2.0.CO;2.

——, J. Dudhia, and D. R. Stauffer, 1994: A description of the Fifth-generation Penn State/NCAR Mesoscale Model (MM5). NCAR Tech. Note NCAR/TN-398+STR, 121 pp., doi:10.5065/D60Z716B.

Gronewold, A. D., A. H. Clites, J. P. Smith, and T. S. Hunter, 2013: A dynamic graphical interface for visualizing projected, measured, and reconstructed surface water elevations on the earth's largest lakes. *Environ. Modell. Software*, **49**, 34–39, doi:10.1016/j.envsoft.2013.07.003.

——, and Coauthors, 2015: Impacts of extreme 2013–2014 winter conditions on Lake Michigan's fall heat content, surface temperature, and evaporation. *Geophys. Res. Lett.*, **42**, 3364–3370, doi:10.1002/2015GL063799.

Gu, H., J. Jin, Y. Wu, M. B. Ek, and Z. M. Subin, 2015: Calibration and validation of lake surface temperature simulations with the coupled WRF-lake model. *Climatic Change*, **129**, 471–483, doi:10.1007/s10584-013-0978-y.

Gula, J., and W. R. Peltier, 2012: Dynamical downscaling over the Great Lakes basin of North America using the WRF regional climate model: The impact of the Great Lakes system on regional greenhouse warming. *J. Climate*, **25**, 7723–7742, doi:10.1175/JCLI-D-11-00388.1.

Harris, I., P. D. Jones, T. J. Osborn, and D. H. Lister, 2014: Updated high-resolution grids of monthly climatic observations—The CRU TS3.10 dataset. *Int. J. Climatol.*, **34**, 623–642, doi:10.1002/joc.3711.

Holtslag, A. A. M., E. I. F. De Bruijn, and H.-L. Pan, 1990: A high resolution air mass transformation model for short-range weather forecasting. *Mon. Wea. Rev.*, **118**, 1561–1575, doi:10.1175/1520-0493(1990)118<1561:AHRAMT>2.0.CO;2.

Hostetler, S. W., G. T. Bates, and F. Giorgi, 1993: Interactive coupling of a lake thermal model with a regional climate model. *J. Geophys. Res.*, **98**, 5045–5057, doi:10.1029/92JD02843.

Huang, A., Y. R. Rao, Y. Lu, and J. Zhao, 2010: Hydrodynamic modeling of Lake Ontario: An intercomparison of three models. *J. Geophys. Res.*, **115**, C12076, doi:10.1029/2010JC006269.

——, ——, and W. Zhang, 2012: On recent trends in atmospheric and limnological variables in Lake Ontario. *J. Climate*, **25**, 5807–5816, doi:10.1175/JCLI-D-11-00495.1.

Hunter, T. S., A. H. Clites, K. B. Campbell, and A. D. Gronewold, 2015: Development and application of a North American Great Lakes hydrometeorological database—Part I: Precipitation, evaporation, runoff, and air temperature. *J. Great Lakes Res.*, **41**, 65–77, doi:10.1016/j.jglr.2014.12.006.

IPCC, 2013: *Climate Change 2013: The Physical Science Basis.* T. F. Stocker et al., Eds., Cambridge University Press, 1535 pp., doi:10.1017/CBO9781107415324.

Kiehl, J. T., J. J. Hack, G. B. Bonan, B. A. Boville, B. P. Briegleb, D. L. Williamson, and P. J. Rasch, 1996: Description of the NCAR Community Climate Model (CCM3). NCAR Tech. Note NCAR/TN-420+STR, 152 pp., doi:10.5065/D6FF3Q99.

Lenters, J. D., 2004: Trends in the Lake Superior water budget since 1948: A weakening seasonal cycle. *J. Great Lakes Res.*, **30** (Suppl.), 20–40, doi:10.1016/S0380-1330(04)70375-5.

——, J. B. Anderton, P. D. Blanken, C. Spence, and A. E. Suyker, 2013: Assessing the impacts of climate variability and change on Great Lakes evaporation: Implications for water levels and the need for a coordinated observation network. Great Lakes Integrated Sciences and Assessments Center Project Rep., 11 pp. [Available online at http://www.glisaclimate.org/media/GLISA_Lake_Evaporation.pdf.]

Lipscomb, W. H., and E. C. Hunke, 2004: Modeling sea ice transport using incremental remapping. *Mon. Wea. Rev.*, **132**, 1341–1354, doi:10.1175/1520-0493(2004)132<1341:MSITUI>2.0.CO;2.

——, ——, W. Maslowski, and J. Jakacki, 2007: Ridging, strength, and stability in high-resolution sea ice models. *J. Geophys. Res.*, **112**, C03S91, doi:10.1029/2005JC003355.

Lofgren, B. M., 2004: A model for simulation of the climate and hydrology of the Great Lakes basin. *J. Geophys. Res.*, **109**, D18108, doi:10.1029/2004JD004602.

——, 2014: Simulation of atmospheric and lake conditions in the Laurentian Great Lakes region using the Coupled Hydrosphere–Atmosphere Research Model (CHARM). NOAA Tech. Memo. GLERL-165, 23 pp. [Available online at https://www.glerl.noaa.gov/pubs/tech_reports/glerl-165/tm-165.pdf.]

Masson, S., P. Terray, G. Madec, J.-J. Luo, T. Yamagata, and K. Takahashi, 2012: Impact of intra-daily SST variability on ENSO characteristics in a coupled model. *Climate Dyn.*, **39**, 681–707, doi:10.1007/s00382-011-1247-2.

Maykut, G. A., and N. Untersteiner, 1971: Some results from a time-dependent thermodynamic model of sea ice. *J. Geophys. Res.*, **76**, 1550–1575, doi:10.1029/JC076i006p01550.

Mellor, G. L., and T. Yamada, 1982: Development of a turbulence closure model for geophysical fluid problems. *Rev. Geophys.*, **20**, 851–875, doi:10.1029/RG020i004p00851.

NCEI, 2013: State of the climate: National overview—Annual 2012. NOAA. [Available online at https://www.ncdc.noaa.gov/sotc/national/201213.]

Notaro, M., A. Zarrin, S. Vavrus, and V. Bennington, 2013: Simulation of heavy lake-effect snowstorms across the Great Lakes basin by RegCM4: Synoptic climatology and variability. *Mon. Wea. Rev.*, **141**, 1990–2014, doi:10.1175/MWR-D-11-00369.1.

——, V. Bennington, and S. Vavrus, 2015: Dynamically downscaled projections of lake-effect snow in the Great Lakes basin. *J. Climate*, **28**, 1661–1684, doi:10.1175/JCLI-D-14-00467.1.

O'Reilly, C. M., and Coauthors, 2015: Rapid and highly variable warming of lake surface waters around the globe. *Geophys. Res. Lett.*, **42**, 10 773–10 781, doi:10.1002/2015GL066235.

Pal, J. S., E. E. Small, and E. A. B. Eltahir, 2000: Simulation of regional-scale water and energy budgets: Representation of subgrid cloud and precipitation processes within RegCM. *J. Geophys. Res.*, **105**, 29 579–29 594, doi:10.1029/2000JD900415.

——, and Coauthors, 2007: Regional climate modeling for the developing world: The ICTP RegCM3 and RegCNET. *Bull. Amer. Meteor. Soc.*, **88**, 1395–1409, doi:10.1175/BAMS-88-9-1395.

Patterson, J. C., and P. F. Hamblin, 1988: Thermal simulation of a lake with winter ice cover. *Limnol. Oceanogr.*, **33**, 323–338, doi:10.4319/lo.1988.33.3.0323.

Rao, Y. R., and D. J. Schwab, 2007: Transport and mixing between the coastal and offshore waters in the Great Lakes: A review. *J. Great Lakes Res.*, **33**, 202–218, doi:10.3394/0380-1330(2007)33[202:TAMBTC]2.0.CO;2.

Reynolds, R. W., T. M. Smith, C. Liu, D. B. Chelton, K. S. Casey, and M. G. Schlax, 2007: Daily high-resolution-blended analyses for sea surface temperature. *J. Climate*, **20**, 5473–5496, doi:10.1175/2007JCLI1824.1.

Rothrock, D. A., 1975: The energetics of the plastic deformation of pack ice by ridging. *J. Geophys. Res.*, **80**, 4514–4519, doi:10.1029/JC080i033p04514.

Schwab, D. J., and K. W. Bedford, 1994: Initial implementation of the Great Lakes Forecasting System: A real-time system for predicting lake circulation and thermal structure. *Water Pollut. Res. J. Canada*, **29**, 203–220.

——, G. A. Leshkevich, and G. C. Muhr, 1992: Satellite measurements of surface water temperature in the Great Lakes: Great

Lakes Coastwatch. *J. Great Lakes Res.*, **18**, 247–258, doi:10.1016/S0380-1330(92)71292-1.

Shore, J. A., 2009: Modelling the circulation and exchange of Kingston basin and Lake Ontario with FVCOM. *Ocean Modell.*, **30**, 106–114, doi:10.1016/j.ocemod.2009.06.007.

Smagorinsky, J., 1963: General circulation experiments with the primitive equations: I. The basic experiment. *Mon. Wea. Rev.*, **91**, 99–164, doi:10.1175/1520-0493(1963)091<0099: GCEWTP>2.3.CO;2.

Song, Y., F. H. M. Semazzi, L. Xie, and L. J. Ogallo, 2004: A coupled regional climate model for the Lake Victoria basin of East Africa. *Int. J. Climatol.*, **24**, 57–75, doi:10.1002/joc.983.

Spence, C., P. D. Blanken, J. D. Lenters, and N. Hedstrom, 2013: The importance of spring and autumn atmospheric conditions for the evaporation regime of Lake Superior. *J. Hydrometeor.*, **14**, 1647–1658, doi:10.1175/JHM-D-12-0170.1.

Steiner, A. L., J. S. Pal, S. A. Rauscher, J. L. Bell, N. S. Diffenbaugh, A. Boone, L. C. Sloan, and F. Giorgi, 2009: Land surface coupling in regional climate simulations of the West African monsoon. *Climate Dyn.*, **33**, 869–892, doi:10.1007/s00382-009-0543-6.

Subin, Z. M., W. J. Riley, and D. Mironov, 2012: An improved lake model for climate simulations: Model structure, evaluation, and sensitivity analyses in CESM1. *J. Adv. Model. Earth Syst.*, **4**, M02001, doi:10.1029/2011MS000072.

Thorndike, A. S., D. A. Rothrock, G. A. Maykut, and R. Colony, 1975: The thickness distribution of sea ice. *J. Geophys. Res.*, **80**, 4501–4513, doi:10.1029/JC080i033p04501.

Titze, D. J., and J. A. Austin, 2014: Winter thermal structure of Lake Superior. *Limnol. Oceanogr.*, **59**, 1336–1348, doi:10.4319/lo.2014.59.4.1336.

Terray, P., K. Kamala, S. Masson, G. Madec, A. K. Sahai, J.-J. Luo, and T. Yamagata, 2012: The role of the intra-daily SST variability in the Indian monsoon variability and monsoon–ENSO–IOD relationships in a global coupled model. *Climate Dyn.*, **39**, 729–754, doi:10.1007/s00382-011-1240-9.

Turuncoglu, U. U., G. Giuliani, N. Elguindi, and F. Giorgi, 2013: Modelling the Caspian Sea and its catchment area using a coupled regional atmosphere–ocean model (RegCM4–ROMS): Model design and preliminary results. *Geosci. Model Dev.*, **6**, 283–299, doi:10.5194/gmd-6-283-2013.

Van Cleave, K., J. D. Lenters, J. Wang, and E. M. Verhamme, 2014: A regime shift in Lake Superior ice cover, evaporation, and water temperature following the warm El Niño winter of 1997–1998. *Limnol. Oceanogr.*, **59**, 1889–1898, doi:10.4319/lo.2014.59.6.1889.

Wang, G., M. Yu, J. S. Pal, R. Mei, G. B. Bonan, S. Levis, and P. E. Thornton, 2016: On the development of a coupled regional climate–vegetation model RCM–CLM–CN–DV and its validation in tropical Africa. *Climate Dyn.*, **46**, 515–539, doi:10.1007/s00382-015-2596-z.

Wang, J., H. Hu, D. Schwab, G. Leshkevich, D. Beletsky, N. Hawley, and A. Clites, 2010: Development of the Great Lakes Ice-Circulation Model (GLIM): Application to Lake Erie in 2003–2004. *J. Great Lakes Res.*, **36**, 425–436, doi:10.1016/j.jglr.2010.04.002.

——, X. Bai, H. Hu, A. Clites, M. Colton, and B. Lofgren, 2012: Temporal and spatial variability of Great Lakes ice cover, 1973–2010. *J. Climate*, **25**, 1318–1329, doi:10.1175/2011JCLI4066.1.

Wei, J., P. Malanotte-Rizzoli, E. A. B. Eltahir, P. Xue, and D. Xu, 2014: Coupling of a regional atmospheric model (RegCM3) and a regional oceanic model (FVCOM) over the Maritime Continent. *Climate Dyn.*, **43**, 1575–1594, doi:10.1007/s00382-013-1986-3.

Williamson, J., 1854: *The Inland Seas of North America; and, the Natural and Industrial Productions of Canada with the Real Foundations for Its Future Prosperity*. H. Ramsay, 78 pp.

Xue, P., and E. A. B. Eltahir, 2015: Estimation of the heat and water budgets of the Persian (Arabian) Gulf using a regional climate model. *J. Climate*, **28**, 5041–5062, doi:10.1175/JCLI-D-14-00189.1.

——, C. Chen, R. C. Beardsley, and R. Limeburner, 2011: Observing system simulation experiments with ensemble Kalman filters in Nantucket Sound, Massachusetts. *J. Geophys. Res.*, **116**, C01011, doi:10.1029/2010JC006428.

——, ——, and ——, 2012: Observing system simulation experiments of dissolved oxygen monitoring in Massachusetts Bay. *J. Geophys. Res.*, **117**, C05014, doi:10.1029/2011JC007843.

——, E. A. B. Eltahir, P. Malanotte-Rizzoli, and J. Wei, 2014: Local feedback mechanisms of the shallow water region around the Maritime Continent. *J. Geophys. Res. Oceans*, **119**, 6933–6951, doi:10.1002/2013JC009700.

——, D. J. Schwab, and S. Hu, 2015: An investigation of the thermal response to meteorological forcing in a hydrodynamic model of Lake Superior. *J. Geophys. Res. Oceans*, **120**, 5233–5253, doi:10.1002/2015JC010740.

Zeng, X., M. Zhao, and R. E. Dickinson, 1998: Intercomparison of bulk aerodynamic algorithms for the computation of sea surface fluxes using TOGA COARE and TAO data. *J. Climate*, **11**, 2628–2644, doi:10.1175/1520-0442(1998)011<2628: IOBAAF>2.0.CO;2.

Zhang, G. J., V. Ramanathan, and M. J. McPhaden, 1995: Convection–evaporation feedback in the equatorial Pacific. *J. Climate*, **8**, 3040–3051, doi:10.1175/1520-0442(1995)008<3040: CEFITE>2.0.CO;2.

Zhong, Y., M. Notaro, S. J. Vavrus, and M. J. Foster, 2016: Recent accelerated warming of the Laurentian Great Lakes: Physical drivers. *Limnol. Oceanogr.*, **61**, 1762–1786, doi:10.1002/lno.10331.